Atmospheric Research 122 (2013) 310–335

Contents lists available at SciVerse ScienceDirect

Atmospheric Research

journal homepage: www.elsevier.com/locate/atmos

Orographic effects on heavy rainfall events over northeastern Taiwan during the northeasterly monsoon season

Ching-Sen Chen [a,*], Yuh-Lang Lin [b], Hui-Ting Zeng [a], Chih-Ying Chen [a], Che-Ling Liu [a]

[a] Institute of Atmospheric Physics, National Central University, Chung-Li, 320 Taiwan
[b] Department of Physics and Department of Energy and Environmental Systems, NC A&T State University, Greensboro, NC 27411 USA

ARTICLE INFO

Article history:
Received 3 November 2011
Received in revised form 30 August 2012
Accepted 4 October 2012
Available online 3 November 2012

Keywords:
Orographic effects
heavy rainfall
northeasterly monsoon

ABSTRACT

The effects of orographic lifting and blocking on a heavy rainfall event with an accumulation of 631.5 mm on 11 October 2009 over the Lan-Yang Plain (LYP) in northeastern Taiwan during the northeasterly monsoon season were studied by performing observational data analyses and numerical simulations using the Weather Research and Forecasting (WRF) model. The synoptic environment included a low-level easterly wind over the East China Sea and a southeasterly wind over the western North Pacific Ocean which produced convergence areas leading to the heavy rainfall event. The mesoscale features and the orographic lifting and blocking effects on the production and maintenance of the heavy orographic rainfall without the direct influence of the typhoon's circulations during the northeasterly monsoon season in fall were first investigated here. Due to orographic blocking on the prevailing easterly wind over the western LYP, the induced near-surface northeasterly flow containing moist airstream was lifted over the windward (south) side of the LYP and rainfall was enhanced in situ. Meanwhile, the precipitating system was embedded in a weak middle-level flow with the wind reversing its direction over the windward side of the LYP, resulting in a quasi-stationary system over the slope area. Furthermore, the prevailing easterly wind ascended over the coastal slope south of the LYP and enhanced the rainfall there. In addition, the approaching east–west oriented rainband from southeast Taiwan also strengthened the rainfall intensity over northeastern Taiwan. Two sensitivity tests were performed to examine the effect of the orographic lifting of the moist airstream on the production of heavy rainfall. The sensitivity experiment with Taiwan's topography removed (the NT run) shows that the simulated accumulated rainfall over northeastern Taiwan was less than 50 mm in one day, much less than in the control run (CR run). In the NT run, the low-level convergence over northeastern Taiwan produced by the synoptic circulations and the simulated rainband still approaching northeastern Taiwan, are similar to the CR run. Another sensitivity experiment replacing the LYP with a plateau (the PL run) shows that the accumulated daily rainfall over the slope south of the LYP was reduced by ~250 mm compared to the CR run. The reduction of rainfall was caused by lifting relatively less moist air over the slope south of the LYP. These sensitivity tests indicate that the amount of low-level moisture and the orographic effects are equally important for the formation and maintenance of heavy rainfall over northeastern Taiwan under a favorable environment.

1. Introduction

It is well known that orography plays an important role in the formation, enhancement and maintenance of heavy rainfall under different synoptic situations over Taiwan (Lin,

* Corresponding author. Tel.: +886 3 4220270; fax: +886 3 4256841.
E-mail address: tchencs@atm.ncu.edu.tw (C.-S. Chen).

0169-8095/$ – see front matter © 2012 Elsevier B.V. All rights reserved.
http://dx.doi.org/10.1016/j.atmosres.2012.10.008

2007; Yen et al., 2011; Federico et al., 2009; Mastrangelo et al., 2011; Feng and Wang Chen, 2011 among others). In particular, during the Mei-Yu (15 May 15 June) and Post Mei-Yu seasons (∽16 June ∽ 30 June), the rainfall associated with the Mei-Yu front and the embedded mesoscale convective systems (MCSs) was often enhanced dramatically by the Central Mountain Range (CMR) (Lin and Chen, 2002; Chen et al., 2005, 2007a, 2010a, 2010b, 2011; Li et al., 1997, 2011 among others). In October, the northeasterly monsoon prevailing over Taiwan (see Fig. 1a and b for

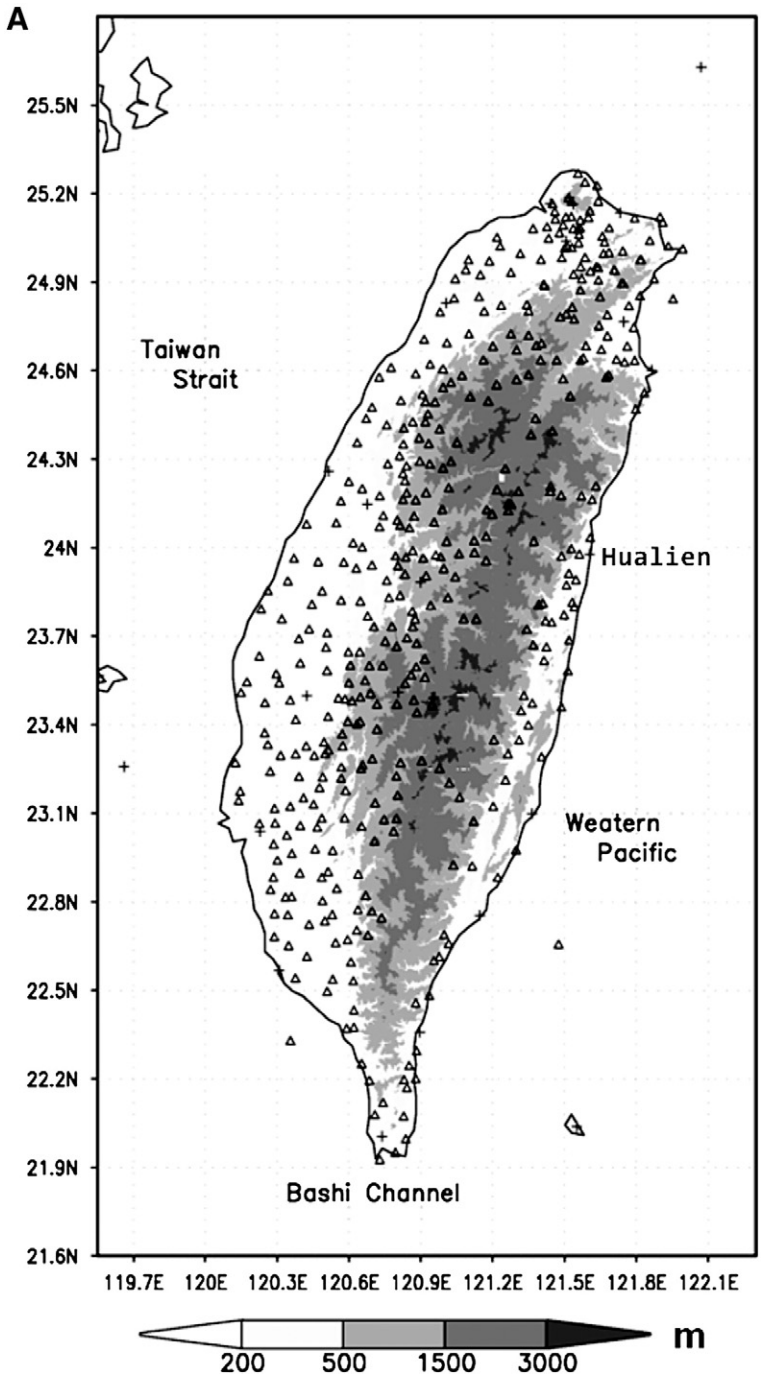

Fig. 1. (A) The topography of Taiwan. The gray scale shows terrain elevations in meters. The triangles and crosses represent the Automatic Rainfall and Meteorological Telemetry System and conventional stations, respectively. (B) Same as (A) but for northeastern Taiwan. The Wu-Fen Shan Doppler radar is indicated by a star symbol. LYP represents Lan-Yang Plain. The locations for conventional station Ilan and Suao are also shown. (C) Same as (B) but for a sensitivity test through the modification of the Lan-Yang Plain (LYP) to a plateau (the PL run).

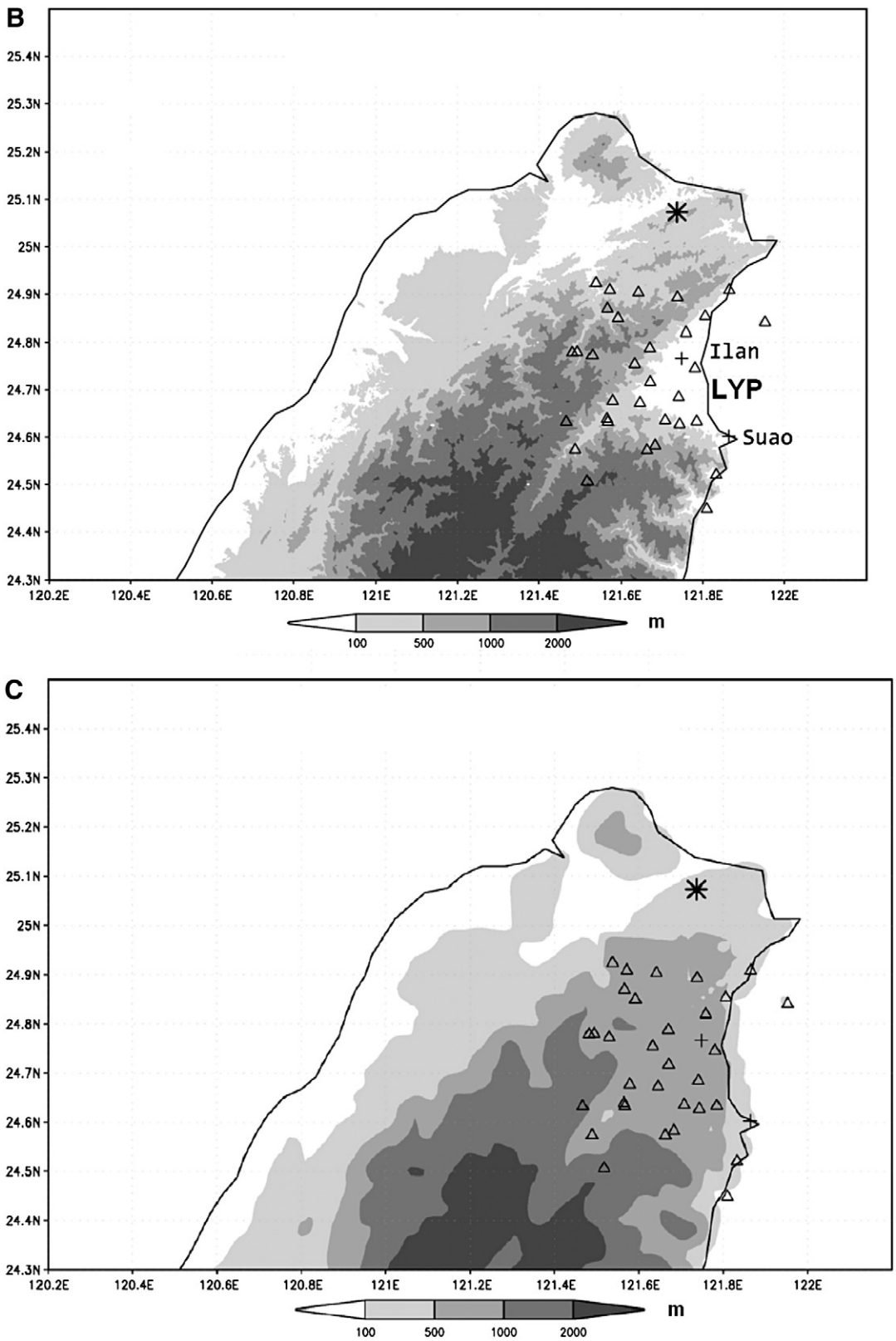

Fig. 1 (*continued*).

the topography) often contained potentially unstable and low-level moist air (Chen and Chen, 2003). The windward slope of northeastern Taiwan frequently experiences heavy rainfall due to its steep terrain (Chen et al., 2007b). Over northeastern Taiwan, the Lan-Yang Plain (LYP) is surrounded by mountains except on its eastern side, which is open to the western North Pacific Ocean (Fig. 1B). Moist airstream, which can be easily transported into the LYP by the prevailing northeasterly monsoon flow, is lifted by the mountains, and can generate heavy rainfall or enhance the pre-existing precipitating system embedded in the monsoon current.

Over northeastern Taiwan during the fall season, the passage of frontal systems also enhances rainfall (Chen and Chen, 2003). In addition, typhoons occur frequently during the fall season and usually migrate from the western North Pacific Ocean westward across Taiwan or its vicinity. Wu et al. (2009) examined a heavy rainfall event (23–26 October 1998) which produced a 3-day accumulated rainfall of over 1200 mm over the mountainous area of the southern side of the LYP, when Typhoon Babs moved from the northeastern South China Sea (SCS) to the Taiwan Strait. The low-level convergence from the interaction of Babs's outer circulation and the northeasterly monsoon was responsible for the production of enhanced rainfall over the entire region of the LYP, including the western and southern mountains of the LYP (Fig. 13 of Wu et al., 2009). Due to the strong low-level wind (~ 15 m s $^{-1}$, Fig. 3B of Wu et al., 2009), the orographic lifting effect was evident over the slope areas in northeastern Taiwan. The 3-day accumulated rainfall was found in the slope area south of the LYP and west of the LYP. The accumulated rainfall over the western slope of the LYP was about 60% of that over the southern slope (Fig. 3A of Wu et al., 2009). A question that may be asked is the following: if a typhoon over the northeastern SCS moves away from Taiwan in a westward direction instead of moving toward the Taiwan Strait during the northeasterly monsoon season, could the heavy rainfall occur in northeastern Taiwan? If it does, what is the main mechanism for producing the heavy rainfall? In this study, we will try to answer these questions.

A slow or impeded movement of the convective system is one of ingredients for producing heavy orographic rainfall (Lin, 2007). The propagation of an orographically-induced MCS may be controlled by the moist Froude number which may be defined as $F_w = U/(N_w \cdot h)$ (Chu and Lin, 2000; also see Lin, 2007 for a review), where U is the upstream basic flow speed perpendicular to the mountain range (approximately easterly flow for the current case), N_w is the moist Brunt-Väisälä frequency, and h is the mountain height. Chu and Lin (2000) proposed that if F_w is around 0.5 (their Regime II), the orographically-induced mesoscale convective cells may develop and persist and remain quasi-stationary over the mountain top and slope areas. Over northeastern Taiwan in October, Zeng (2011)[1] approximately estimated that $U = 8$ m s^{-1}, $N_w = 0.006$ s^{-1}, and $h = 2$ km. This gives $F_w = 0.55$ over the mountainous area south of the LYP (Fig. 1B) and falls into Regime II of Chu and Lin (2000). Thus we may expect the rainfall system to form and be maintained over the mountainous areas under such a large-scale environment.

In the low Froude-number flow regime, the orographically blocked low-level easterly wind tends to produce rainfall in a near-surface northeasterly wind near northeastern Taiwan (Lin, 2007). Therefore, we may hypothesize that the heavy rainfall over the mountain slope south of the LYP is mainly generated by the orographic lifting on the low-level northeasterly moist airstream along the windward (south) side of the LYP and by the prevailing easterly wind along the eastern slope of the LYP. The precipitating system becomes quasi-stationary over the mountain slopes under a suitable vertical wind structure.

The objective of this study is to identify the orographic lifting and blocking effects on the generation and maintenance of heavy rainfall over northeastern Taiwan when the monsoonal northeasterlies converge with the southeasterly flows over northeastern Taiwan, without the direct influence of the typhoon's circulations. The mesoscale processes associated with the development and maintenance of the heavy rainfall event under the influence of orography are investigated by the WRF model (Skamarock et al., 2005). In Section 2, we will identify the synoptic and mesoscale environments associated with the 11 October 2009 heavy rainfall event over the LYP by performing observational analyses of the European Centre for Medium-Range Weather Forecasts (ECMWF) data, satellite imagery, radar reflectivity, and rainfall data. The simulation results from the WRF model and the generation and maintenance mechanisms of the heavy rainfall over northeastern Taiwan will be presented in Section 3. The summary is provided in Section 4.

2. Overviews of the heavy rainfall on 11 October 2009

2.1. Observational data analysis

The available observational data include Doppler radar data, conventional surface observations, and Automatic Rainfall and Meteorological Telemetry System (ARMTS; Chen et al., 2007b) data. The temporal and horizontal spatial resolution of Wu-Fen Shan (mountain) radar (Fig. 1B) data is 6 min and 1 km, respectively. In the vertical resolution, the analysis layer is from 1.5 to 9.75 km with a 0.75 km interval. Because the highest peak of the mountains of CMR is higher than 2 km south of 24.5°N, the current analysis is focused on the area north of 24.5°N. Another radar data used in this study is from the Hualien radar (see Fig. 1A for the location). For reconnaissance purposes, both Wu-Fen Shan and Hualien radar data are used. The horizontal resolution is 1 km. The layer composite reflectivity maximum above any 1-km^2 area vertically will be shown in Fig. 5A. Synoptic conditions are depicted from the 1.125 degree ECMWF/Tropical Ocean-Global Atmosphere (EC/TOGA) data.

[1] The author of the MS thesis shown in the reference is also one of the authors of this study.

2.2. Extremely heavy rainfall events over northeastern Taiwan in autumn from 1995 to 2009

In order to examine the role of the orographic lifting and blocking effects on the generation and maintenance of heavy rainfall under the influence of the northeasterly monsoon, 14 extremely heavy rainfall events occurring during the fall over northeastern Taiwan were identified. These events occurred when the synoptic disturbances were at least 500 km away from Taiwan during the period of 1997 to 2009 (Table 1). *Extremely heavy rainfall* is defined by the Central Weather Bureau (CWB) of Taiwan as the following: where the accumulated daily rainfall exceeds 200 mm and at least one rainfall rate per hour greater than 15 mm is recorded by at least one rainfall station. The low-level prevailing wind of 12 out of 14 events was from east-northeast to east-southeast (Zeng, 2011). Most of these 14 cases appeared in early October (Table 1), which is consistent with the period of maximum occurrences of heavy rainfall over northeastern Taiwan (Chen et al., 2007b). Fig. 2A shows the locations of the maximum daily accumulated rainfall associated with these 14 events superimposed on the averaged daily rainfall of all 14 events over northeastern Taiwan. Relatively high rainfall as well as the maximum daily accumulated rainfall associated with all 14 heavy rainfall events is over the slope and mountainous areas south of the LYP. The average rainfall over the western slope areas of the LYP is about 35% of the rainfall in the southern slope and mountainous areas. This ratio is much smaller than that in the events studied by Wu et al. (2009). In other words, orographic lifting over the slope west of the LYP in these 14 cases may not be as evident as in the case studied by Wu et al. (2009). These 14 events are cases with localized heavy rainfall that propose a great challenge to forecasters. Since there were no synoptic disturbances in Taiwan's vicinity for those 14 extremely heavy rainfall events, it may be assumed that the generation and maintenance of heavy rainfall over northern Taiwan associated with these events were mainly forced by the orography (Lin, 2007). We will focus on the event of 11 October 2009 to test our hypothesis on heavy rainfall generation and maintenance over northeastern Taiwan, because the measurements (631.5 mm in one day and 168.5 mm for area averaged rainfall over northeastern Taiwan for this particular case) are the highest ranked among these 14 events (Fig. 2B and Table 1). The ratio of the rainfall over the western slope of the LYP and the mountainous area south of the LYP is about 10%, suggesting a highly localized rainfall distribution. In addition, a westward-movement typhoon over northeastern SCS was present on 11 October 2009 (Fig. 3A). Thus, this particular case offers us an opportunity to examine the orographic lifting and blocking effects on the heavy rainfall event.

Table 1
The date, maximum accumulated daily rainfall (mm) and area average daily rainfall over northeastern Taiwan (mm) from the existing rainfall stations (in parentheses) for 14 heavy rainfall events.

Case		Maximum accumulate daily rainfall (mm)	Areal average daily rainfall (mm) fram the existing rainfall stations (in parentheses)
1	09oct 1996	232	60.3(20)
2	13oct 2000	218	57.3(27)
3	14oct 2000	266.5	65.8(27)
4	13nov 2000	201.5	70.3(26)
5	04oct 2003	326.5	61.1(28)
6	25nov 2003	202	30.5(29)
7	08oct 2005	286	125.6(29)
8	21sep 2006	206	68.7(29)
9	12oct 2007	260.5	42.3(29)
10	13oct 2007	211.5	33.2(26)
11	01nov 2007	314.5	69.7(25)
12	11oct 2009	631.5	168.5(27)
13	12oct 2009	351	116(27)
14	13oct 2009	222.5	60.8(27)

2.3. Synoptic and mesoscale environments for the precipitation system of 11October 2009

At 0200 LST 11 October (1800 UTC 10 October) 2009, the synoptic weather situation from EC/TOGA data shows that a tropical southeast Asian high at 200-hPa level was present over southern China and Taiwan, resulting in a weak divergence over northeastern Taiwan (Zeng, 2011). At the 850-hPa level, a high pressure system extended from east-central China to the East China Sea and a monsoon trough/intertropical convergence zone (ITCZ) stretched over the South China Sea (SCS), the Philippines, and the western North Pacific Ocean (Fig. 3A). Within the monsoon trough, Typhoon Parma was situated over the SCS and headed westward. In the middle troposphere, a mesoscale high pressure center was located over the western Pacific Ocean (Fig. 3A). A southerly flow was situated in northern Taiwan and its vicinity (Fig. 3A). In the low layer, the easterly wind converged with the southeasterly flow associated with the monsoon trough/ITCZ over northeastern Taiwan and its vicinity (Fig. 3A). The upstream low-level airflow in northeastern Taiwan was potentially unstable and conditionally unstable (Fig. 3B); it was moist and persistently transported into northern Taiwan (Fig. 3C). The moist Froude number, as defined in the Introduction, was about 0.6.

The evolution of the surface wind and its virtual potential temperature at Ilan and Suao (see Fig. 1B for the locations) in LYP on 11 October is shown in Fig. 4. Within the LYP, the surface wind came from the northeast while the easterly wind prevailed over the southern coast of LYP. This environment suggests that the orographic blocking by the topography occurred to the west of the LYP. Due to the persistence of rainfall at Ilan, the virtual potential temperature within the LYP was lower than that at the coast. The northeasterly wind speed at Ilan increased after 0500 LST. Concurrently, the increase of northerly wind component at the 950-hPa level after 2000 LST 10 October was present (Fig. 3C). It was apparent that the low-level ascending motion over the slope south (windward side) of the LYP due to orographic lifting would be enhanced. As the low-level wind transports the moist air from the adjacent ocean with a higher virtual potential temperature than that within the LYP, the ascending motion may strengthen precipitation over the slope south of the LYP. On the other hand, the orographic lifting over the slope west of the LYP is not obvious due to the fact that the

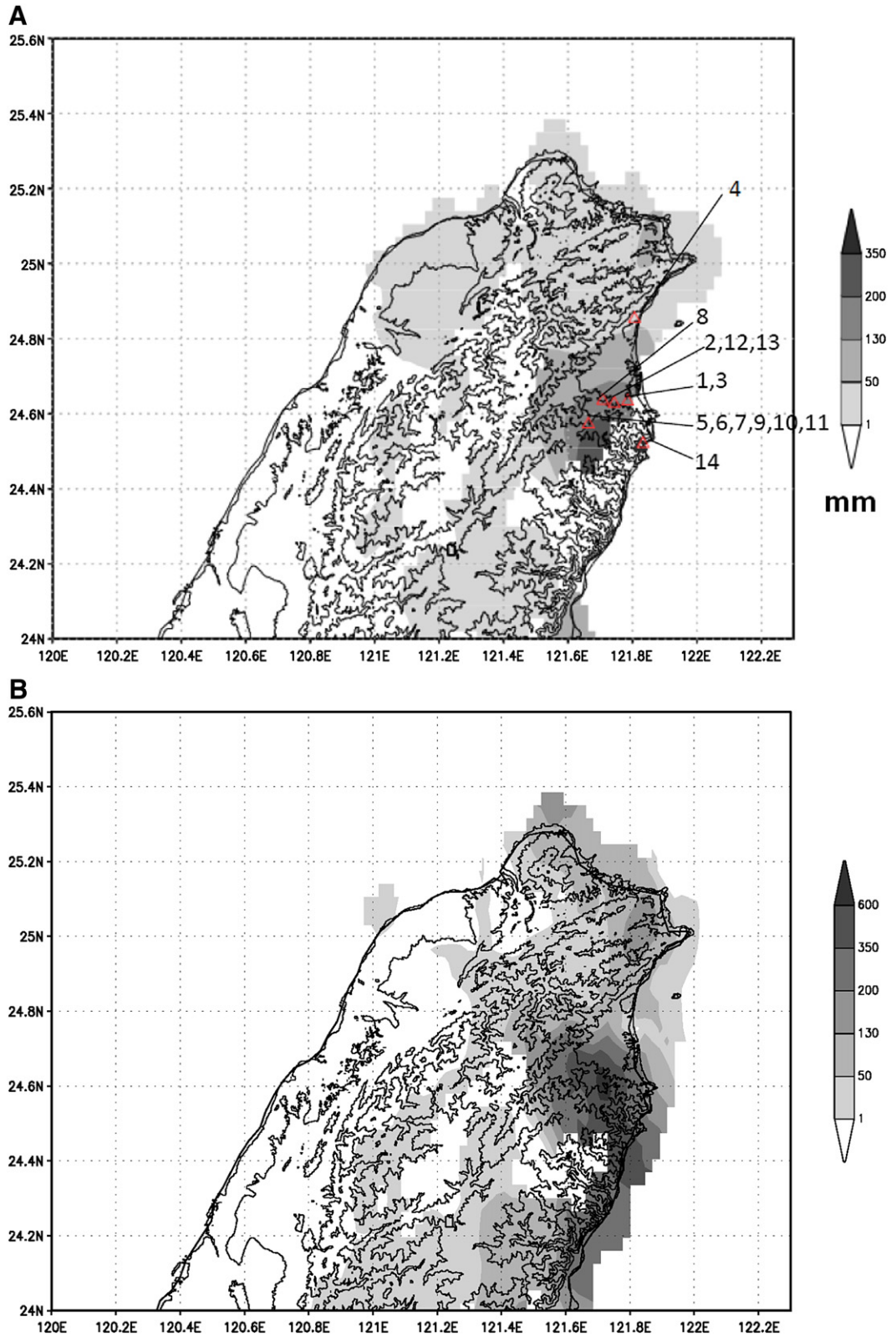

Fig. 2. (A) The averaged daily rainfall from 14 heavy rainfall events (Table 1). Rainfall amount is shown by the gray scale (mm). The location of the maximum daily accumulated rainfall for each event is indicated by the "digital number" in Table 1. Terrain height (solid lines) is 1, 100, 500, 1000, and 2000 m, respectively. (B) The observed daily accumulated rainfall on 11 October 2009. Rainfall amount is shown by the gray scale (mm). Terrain height (solid lines) is 1, 100, 500, 1000, and 2000 m, respectively.

topography is approximately parallel to the low-level wind (Fig. 1B).

Satellite images indicate that an east–west oriented convective cloud system had already developed over the ocean to southeast Taiwan on 10 October. Radar echoes had already appeared over the slope areas of northeastern Taiwan in the early morning of 11 October before the approach of the east–west oriented convective cloud band (Fig. 5A). By 1000 LST 11 October, the east–west oriented cloud band had reached northeastern Taiwan (Fig. 5B). Concurrently, radar echoes had intensified over northern Taiwan (Fig. 5C) as the convective cloud band approached. At 1200 LST, intensive radar echoes occurred over northeastern Taiwan (Fig. 5D). In the afternoon, radar echoes weakened over northeastern Taiwan. However, strong radar echoes were present over the ocean near the northeastern coast (Zeng, 2011).

To illustrate the duration of the heavy rainfall, the occurrence frequency of radar echoes exceeding 20 dBZ over northeastern Taiwan on 11 October is calculated from 6-min radar reflectivity (Fig. 6A). More than 50% of the occurrence frequency with two local maxima appeared over the mountainous area south of the LYP. Near the gentle slopes and to the southeastern coasts of the LYP, more than 40% of occurrence frequency was detected. The maximum frequency of the occurrences of radar echoes exceeding 35 dBZ shifted slightly westward from those exceeding 20 dBZ (Fig. 6A). The third local maximum was near 24.4°N. In order to examine the duration of the radar echoes over the southern slope areas of LYP, we analyzed the temporal evolution of radar echoes (Fig. 6B) along line L1 passing through the maximum occurrence of radar echoes exceeding 20 dBZ (Fig. 6A). The radar echoes are averaged perpendicular to L1 over a distance of about 10 km. Notice that very weak low-level echoes over the LYP may not be detected by the Wu-Fen Shan radar (Fig. 1B).

On 11 October, a series of echoes sustained over the slopes (Fig. 6B) as the prevailing wind transported the moisture toward northeastern Taiwan (Fig. 3C). During the periods of 0230–0430, 0700–1000, 1100–1230, and 1700–1800 (LST), relatively stronger radar echoes occurred in the mountainous area near the maximum accumulated rainfall region (Fig. 6B). In addition, radar echoes moved eastward from the mountains towards the coasts near 0400 and 1230 LST. The upstream moving radar echoes could be due to the additional lifting on the incoming moist air by the eastward movement of the low-level relatively cool air. This hypothesis will be tested in Section 3. Furthermore, radar echoes moved from the adjacent ocean westward towards the mountainous area from 0700 to 0900 LST, while an east–west oriented rainband approached from the ocean to the vicinity of eastern Taiwan at 0600 LST (Fig. 5a). Most of the radar echoes formed and remained over the slopes, confirming the hypothesis that a quasi-stationary rainfall system is necessary for the formation of heavy rainfall.

Rainfall appeared over the southern mountainous areas of the LYP in the early morning at 0200 LST and intensified at 0600 LST (Fig. 7A). Most of the rainfall fell in the mountain area south of the LYP. Much weak rainfall fell in the slope west of the LYP. Rainfall continued over the slope and mountainous areas south of the LYP at 1000 LST (Fig. 7B). The maximum hourly rainfall rate over mountainous areas occurred at 1200 LST (Fig. 7C) as the east–west-oriented rainband developed and approached northeastern Taiwan (Fig. 5). In contrast, rainfall rate over the northern LYP and western slope remained weaker than in the slope and mountainous areas south of the LYP (Fig. 7). The hourly rainfall rate weakened over the slope south of the LYP in the late afternoon but intensified again, especially over the southeast coast of the LYP (Zeng, 2011). Over northeastern Taiwan, rainfall persisted until the next day (not shown). The location of the maximum accumulated rainfall (Fig. 2B) was about 5 km to the northwest of the maximum occurrence of radar echoes exceeding 20 dBZ (Fig. 6A). It could be caused by the transport of hydrometeors due to the easterly winds[2] or by the low spatial resolution of rainfall stations over mountain (Fig. 1B). Most of the accumulated rainfall was over the slope and mountainous area south of the LYP (Fig. 2B). Owing to the weak orographic lifting over the western slope of the LYP (Fig. 1B) from the low-level northeasterly winds (Fig. 4), rainfall over the mountainous areas west of the LYP was significantly less than that in the southern mountainous areas. Consequently, the ratio of the rainfall over the slope west of the LYP to the slope south of the LYP is small. This phenomenon with localized heavy rainfall is quite different from the case studied by Wu et al. (2009).

3. Simulation Results

3.1. Model description and experiment design

The WRF model version 2[3] was employed to help understand the details of the dynamics and physical processes responsible for the heavy rainfall on 11 October 2009. In order to better resolve the synoptic circulations, mesoscale features, and the orographic lifting and blocking effects on the production of heavy rainfall over northeastern Taiwan (Fig. 2B), three nested grids with a horizontal grid spacing of 18 km, 6 km, and 2 km were used. All domains were comprised of 31 vertical levels from the surface to 50 hPa. The moist processes adopted in the model include the subgrid-scale cumulus parameterization of the Kain and Fritsch scheme (1993) in Domains 1 and 2 and the grid-resolvable Goddard microphysics scheme with three-class ice with graupel (Tao et al., 2003). Planetary boundary layer processes were represented by the Mellor-Yamada-Janjic TKE scheme (Janjic, 1996, 2002). The land surface model has five soil layers (Dudhia, 1996). The model was initialized and lateral boundary conditions derived from the EC/TOGA analyses at 1400 LST (0600 UTC) on 10 October 2009 and integrated for 36 h. During the 36 h integration, the lateral boundary conditions were taken from EC/TOGA analyses. In order to examine the orographic effects on the occurrence of the heavy rainfall over southwestern Taiwan, we performed a sensitivity test excluding Taiwan's topography

[2] This is suggested by a reviewer.

[3] WRF model version 2 is adopted because it has been successfully used to study a heavy rainfall event over southwestern Taiwan on 27 and 28 June 2008 (Chen et al., 2011), although the microphysics scheme (Tao et al., 2003) is different from that used in version 2. Recently, Wapler and Lane (2012) used WRF model version 2 to study a case of offshore convection near Darwin, Australia.

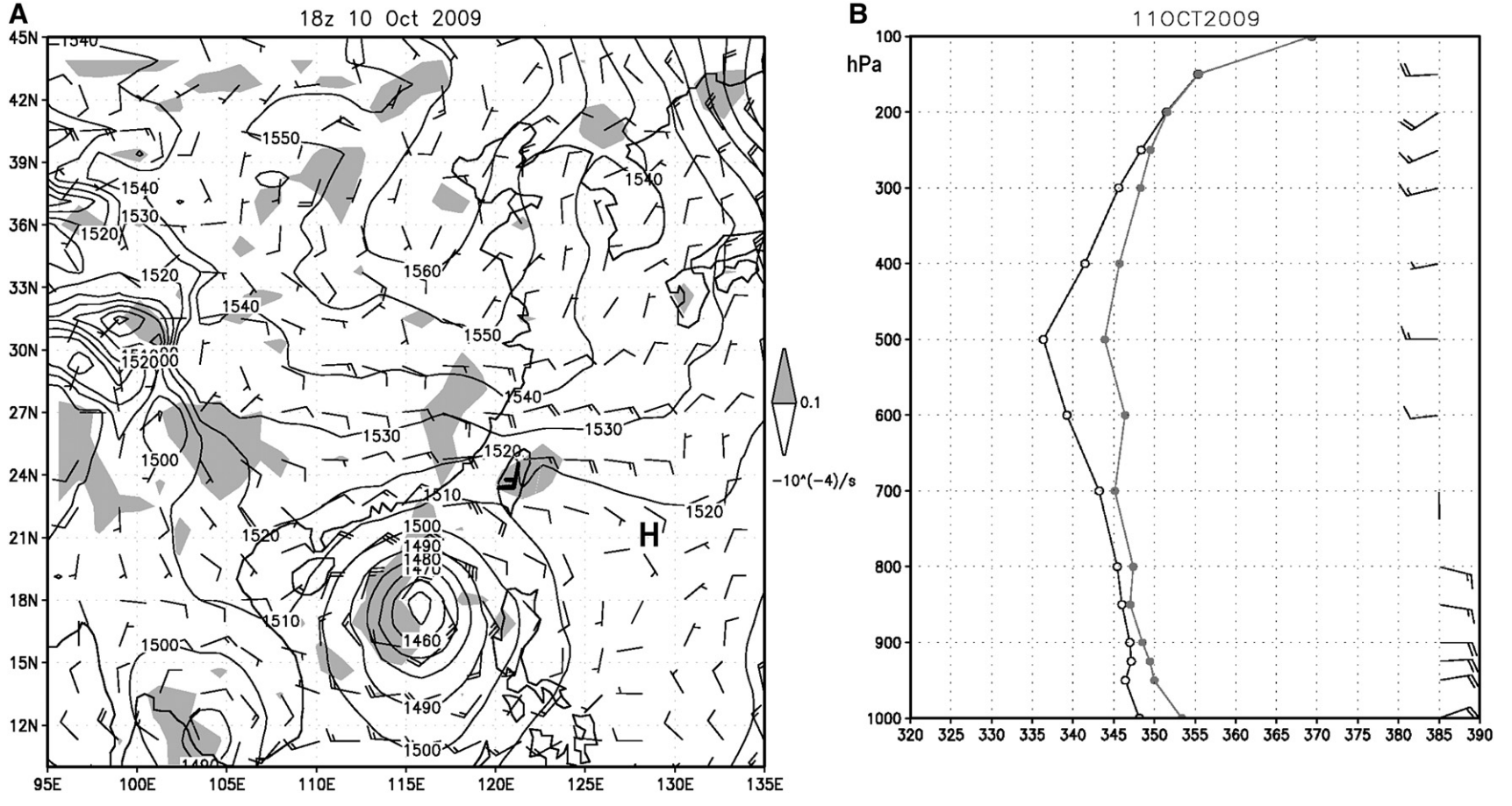

Fig. 3. (A) The 850-hPa synoptic analysis at 0200 LST 11 October 2009 from ECMWF/TOGA data including heights (solid lines, 10 gpm contour interval) and winds (a full bar and a half bar represent 5 and 2.5 m s^{-1}, respectively; also used for other figures). The shaded areas represent the convergence greater than 10^{-5} s^{-1}. The H (~129°E and 21°N) in bold represents the approximate location of a mesoscale high pressure center at the 500-hPa level and the wind in northern Taiwan at the 500-hPa level is represented by a bold wind bar. (B) The profiles for the equivalent potential temperature (open circle in K), the saturated equivalent potential temperature (closed circle in K), and winds at 125°E and 25°N at 0800 LST 11 October 2009 from ECMWF/TOGA data. (C) The 850-hPa wind (in blue) and 925-hPa relative humidity (solid line) at 125 °E and 25 °N and 925-hPa wind (in red) at 121.75°E and 25°N from 0800 LST 10 October to 0800 LST 12 October 2009.

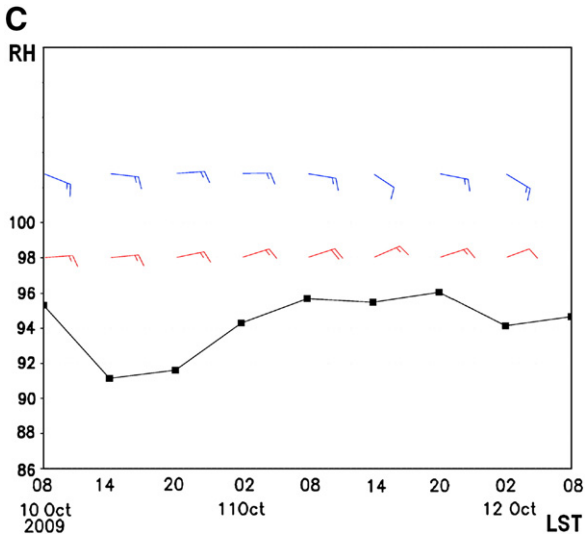

Fig. 3 (*continued*).

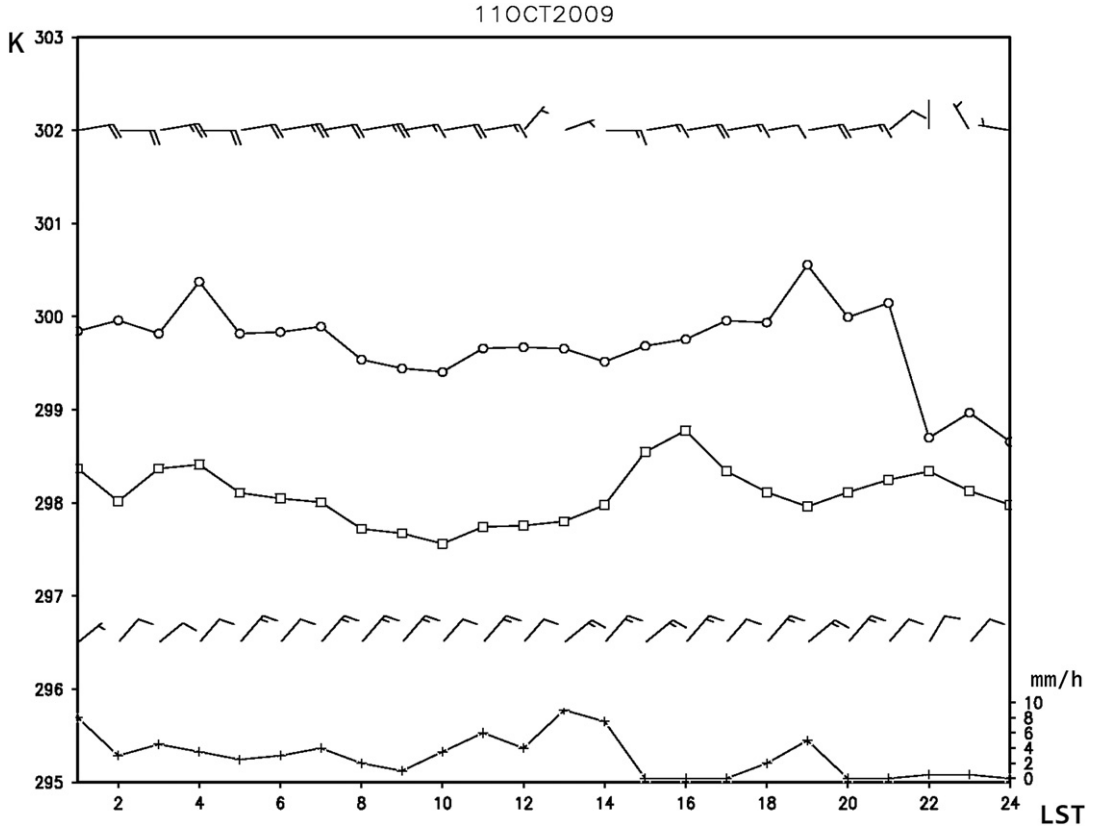

Fig. 4. The variation of surface winds (bottom), virtual potential temperature (square in K), and hourly rainfall rate (solid line in mm h^{-1}) at Ilan and surface winds (top) and virtual potential temperature (circle) at Suao on 11 October 2009. The locations for Ilan and Suao are shown in Fig. 1B.

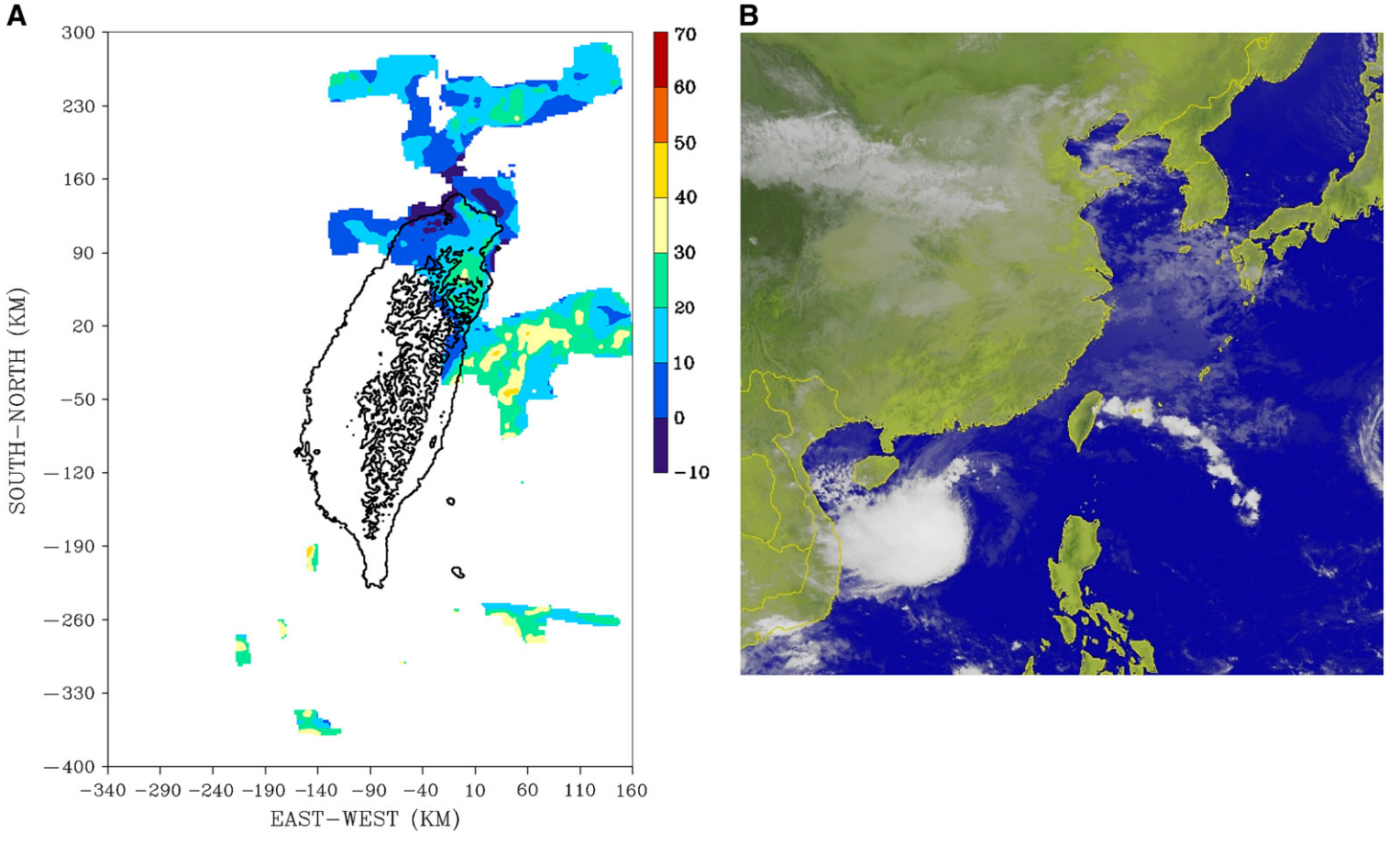

Fig. 5. (A) Composite radar reflectivity (dBZ in color bar) from the Wu-Fen Shan and Hualien radars at 06000 LST 11 October 2009. The horizontal resolution is 1 km. The layer composite reflectivity maximum above any 1-km^2 area vertically is shown. (B) IR image at 1000 LST 11 October 2009. (C) Same as (A) but for 1000 LST. (D) Same as (A) but for 1200 LST.

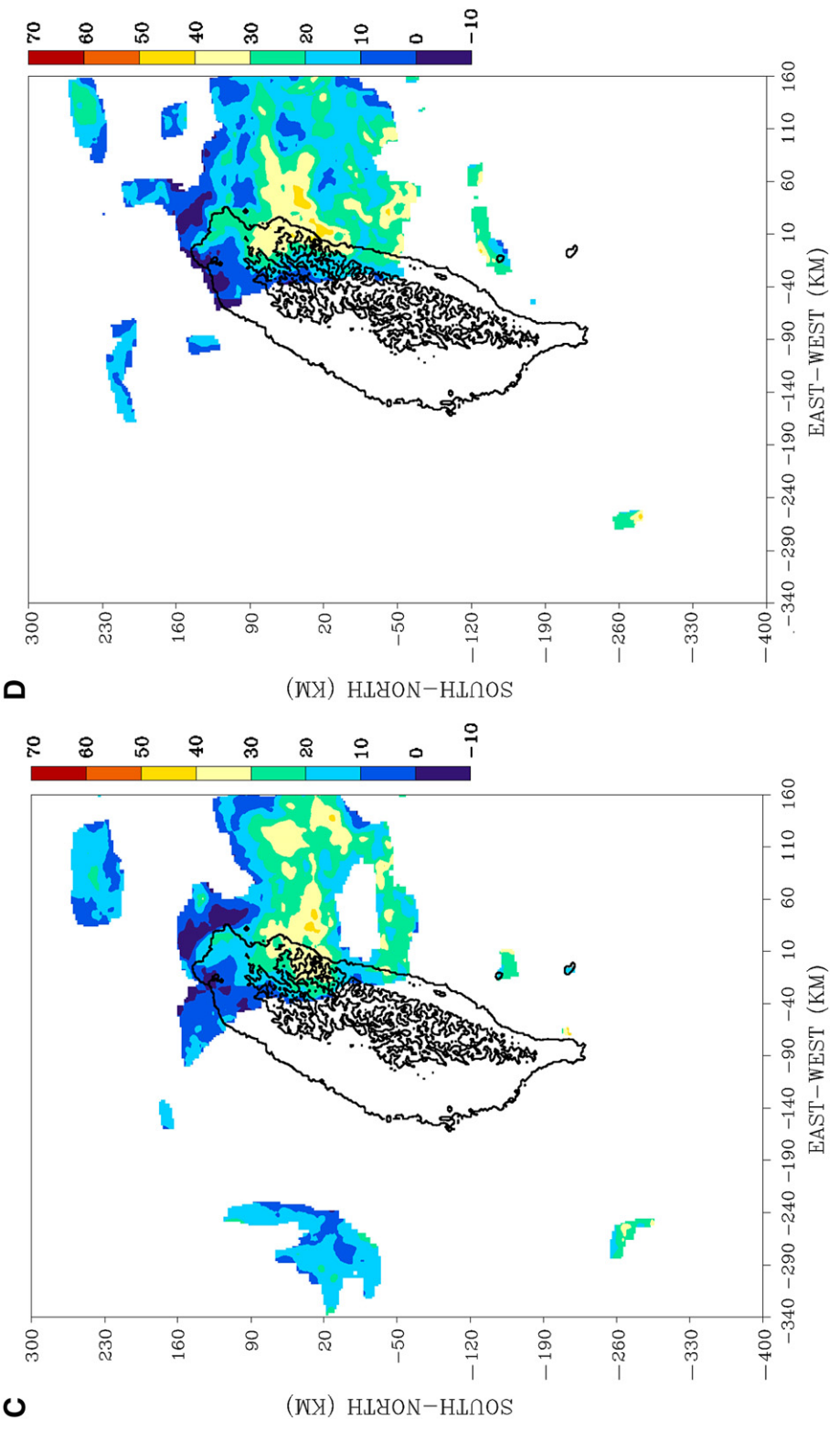

Fig. 5 (*continued*).

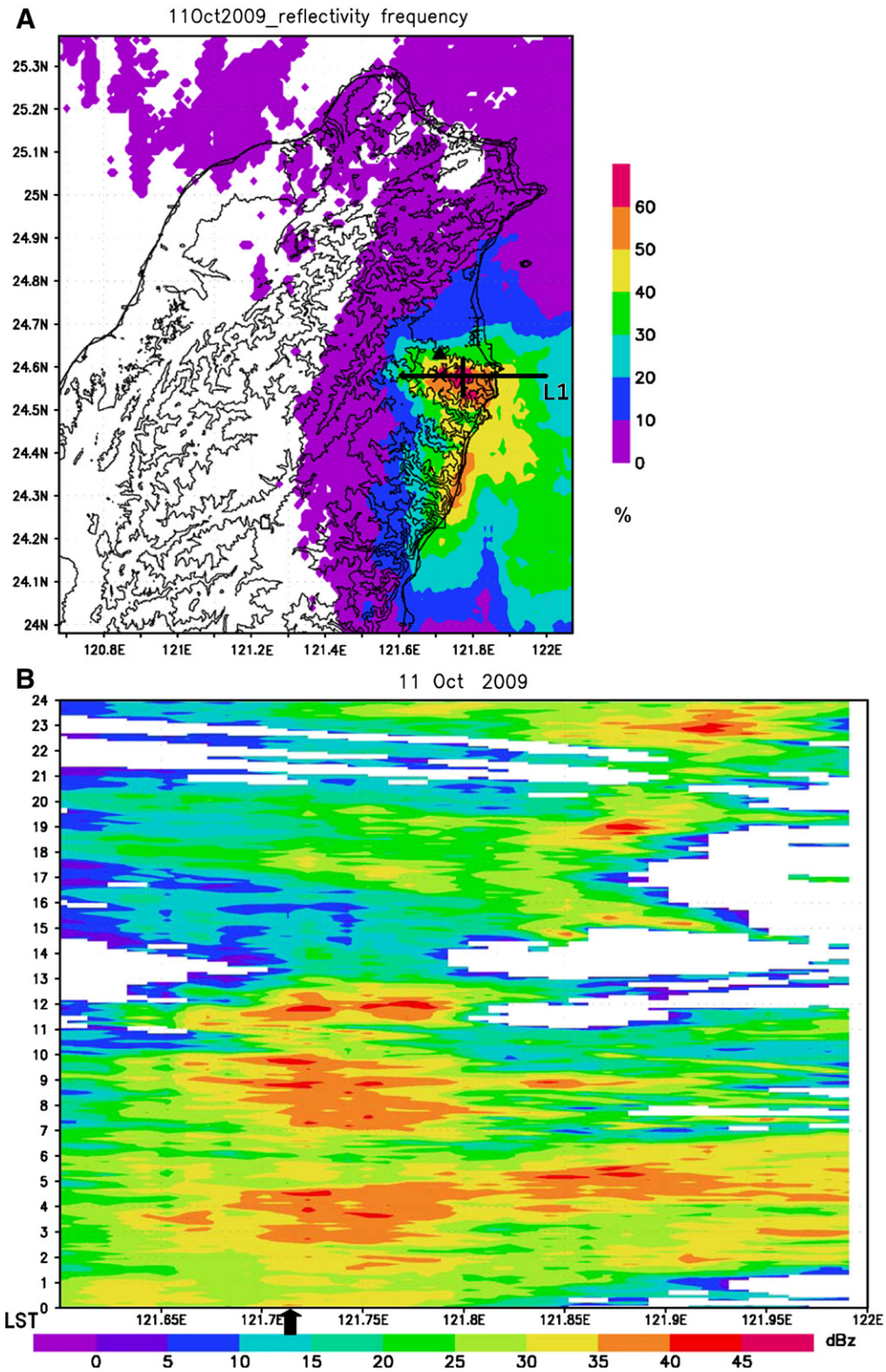

Fig. 6. (A) Frequency (%) of radar reflectivity exceeding 20 dBZ from the Wu-Fen Shan radar on 11 October 2009. Terrain height (solid lines) is 1, 100, 500, 1000, and 2000 m, respectively. The star and triangle represent the approximate locations for maximum frequency of radar reflectivity exceeding 35 dBZ and the maximum accumulated rainfall station, respectively. Line L1 passing through the maximum frequency of radar echoes exceeding 20 dBZ is used in (B). Line perpendicular to L1 indicates averaging width. (B) The temporal evolution of the averaged radar echoes in a 10-km averaged width along L1 in (A). The arrow indicates the approximate location of the maximum accumulated rainfall.

(here after abbreviated as NT run) on 6-km and 2-km grid spacing simulations, while keeping everything else identical to the control run. The procedure of the setup of topography in the NT run was similar to that in Chiao et al. (2004). In order to investigate the influence of the LYP on the production of heavy rainfall on the surrounding sloped areas, another sensitivity test was performed by modifying the LYP to a plateau (here-after abbreviated as PL run) such that an elevation lower than 500 m is roughly parallels the coasts in the LYP (Fig. 1C).

3.2. Simulations of the evolution of precipitation and accumulated rainfall over northeastern Taiwan

The simulated large-scale pattern at 850 hPa obtained from the 18 km grid spacing domain at 0200 LST 11 October is characterized by a high pressure system over east-central China and Typhoon Parma over SCS (Zeng, 2011), similar to observation (Fig. 3a). Low-level easterly winds are simulated upstream of northeastern Taiwan while a northeasterly wind is simulated within the LYP from the 6-km grid spacing (Fig. 8A). These simulated wind fields over northeastern Taiwan are similar to the observations (Fig. 4). The rainfall obtained from the 6-km grid simulation over the slope south of the LYP (Fig. 8A) is slightly weaker than that observed (not shown). Meanwhile, an east–west oriented rainband appears over the east coast where the convergence area is located. The convergence is formed between the prevailing easterly wind and the southeasterly wind associated with the monsoon trough/ITCZ over the western Pacific Ocean (Fig. 8A), consistent with observation (Fig. 3A). In addition, the convergence produced by the deceleration of the prevailing wind approaching Taiwan also enhances the rainband. The simulated rainfall rate increased over northeastern Taiwan (Fig. 8B) as observed (Fig. 7A). Concurrently, the east–west oriented rainband over the ocean to southeast Taiwan intensified while it moved northward (Fig. 8B).

At 1100 LST, the east–west oriented rainband reached the mountainous areas south of the LYP and a high simulated rainfall rate occurred (Fig. 8C). The arrival time of the rainband over northeastern Taiwan was similar to that observed (Fig. 5B and c), but the heaviest simulated rainfall occurred around 1100 LST (Fig. 8C), an hour earlier than that observed (Fig. 7C). In the afternoon, the simulated rainfall over northeastern Taiwan decreased but strengthened again at 2100 LST (not shown), similar to the observation (Zeng, 2011).

The simulated accumulated rainfall obtained from the 2- km grid spacing model over northeastern Taiwan on 11 October is shown in Fig. 9. The simulated maximum 24 h accumulated rainfall is about 650 mm and it is located approximately 5 km southeast of the observed maximum rainfall (Fig. 2B) and at a higher elevation than that observed. However, the location of the simulated maximum accumulated rainfall is close to the location of maximum occurrence frequency of radar echoes exceeding 20 dBZ (Fig. 6A). The second simulated local 24 h accumulated maximum rainfall is about 18 km south of the simulated maximum rainfall, and it corresponds to a local maximum of the occurrence of radar echoes exceeding 20 dBZ (near 24.4°N in Fig. 6A). Most of the simulated rainfall occurs over the slope south of the LYP, similar to the observed (Fig. 2B).

The temporal evolution of the simulated rainfall obtained from the 2- km grid spacing run along the cross section EF passing through the maximum 24 h accumulated rainfall (Fig. 9), similar to L1 (Fig. 6A) is shown in Fig. 10. The simulated rainfall is averaged perpendicular to EF over a distance of about 10 km. The maximum simulated accumulated daily rainfall is about 4 km east of the observed as illustrated in Fig. 10. Over the maximum simulated rainfall area, most of the simulated rainfall occurred before 1300 LST, consistent with that observed (Fig. 6B). Heavy rainfall occurred from 0700 to 0900 and 1000 to 1130 LST (Fig. 10) which corresponds to the temporal variation of radar echoes from 0700 to 1000 and 1100 to 1230 LST, respectively (Fig. 6B). The simulated high rainfall rate from 1800 to 2100 LST corresponds with the high radar echoes from 1700 to 2000 LST (Fig. 6B). The duration of the simulated rainfall around noon is shorter than the duration of radar echoes around noon. In addition, the weak intensity of the simulated rainfall before 0500 LST is not consistent with the observed high radar echoes before 0430 LST (Fig. 6B). In summary, the persistence of the simulated rainfall over the slope south of the LYP resembles the characteristics of radar echoes (Fig. 6B). Consequently, heavy rainfall occurs over the slope south of the LYP.

3.3. The generation and maintenance mechanisms of heavy rainfall over northeastern Taiwan

Since both the observed and simulated maximum accumulated rainfall were over the slope south of the LYP, we will focus on the rainfall formation and maintenance there. At 0600 LST, the ascending motion near the slope south of the LYP along the cross section AB (Fig. 9) induced by the simulated low-level northeasterly wind generates precipitation over the slope area (Fig. 11A). Consequently, rainfall rate increases dramatically over the slope south of the LYP (Fig. 11a). The persistent lifting of moist air by the northeasterly wind induces high rainfall rate over the slope area along cross section AB at 1000 LST (Fig. 11B). Furthermore, the simulated rainfall is embedded in a weak middle-level flow with the wind reversing its direction over the windward side of the LYP, similar to that observed (Fig. 3A), resulting in a quasi-stationary system over the slope area along the same cross section (Fig. 11A and B).

Besides, the prevailing easterly wind also enhances the ascending motion along the cross section CD (Fig. 9) and strengthens rainfall in a conditionally unstable airstream over the slope area at 0600 LST (Fig. 11C). The incoming airflow with low-level conditional instability is similar to the observed (Fig. 3B). The production of a high rainfall rate from the release of conditional instability near the slope area is also found over southwestern Taiwan during the southwesterly monsoon (Chen et al., 2011). Furthermore, as the simulated rainband approaches northeastern Taiwan (Fig. 8), the persistent lifting of extra moist air by the prevailing wind induces a high rainfall rate over the slope area along cross section CD (Fig. 11D and E). Although heavy rainfall occurs over a windward slope area (near 121.75°E) (Figs. 11C, D and 10), the extension of the simulated rainfall towards the west is evident (Figs. 11C, D, and 10). The persistent formation of rainfall over the windward side of the LYP by the prevailing easterly wind and the induced low-level northeasterly flow

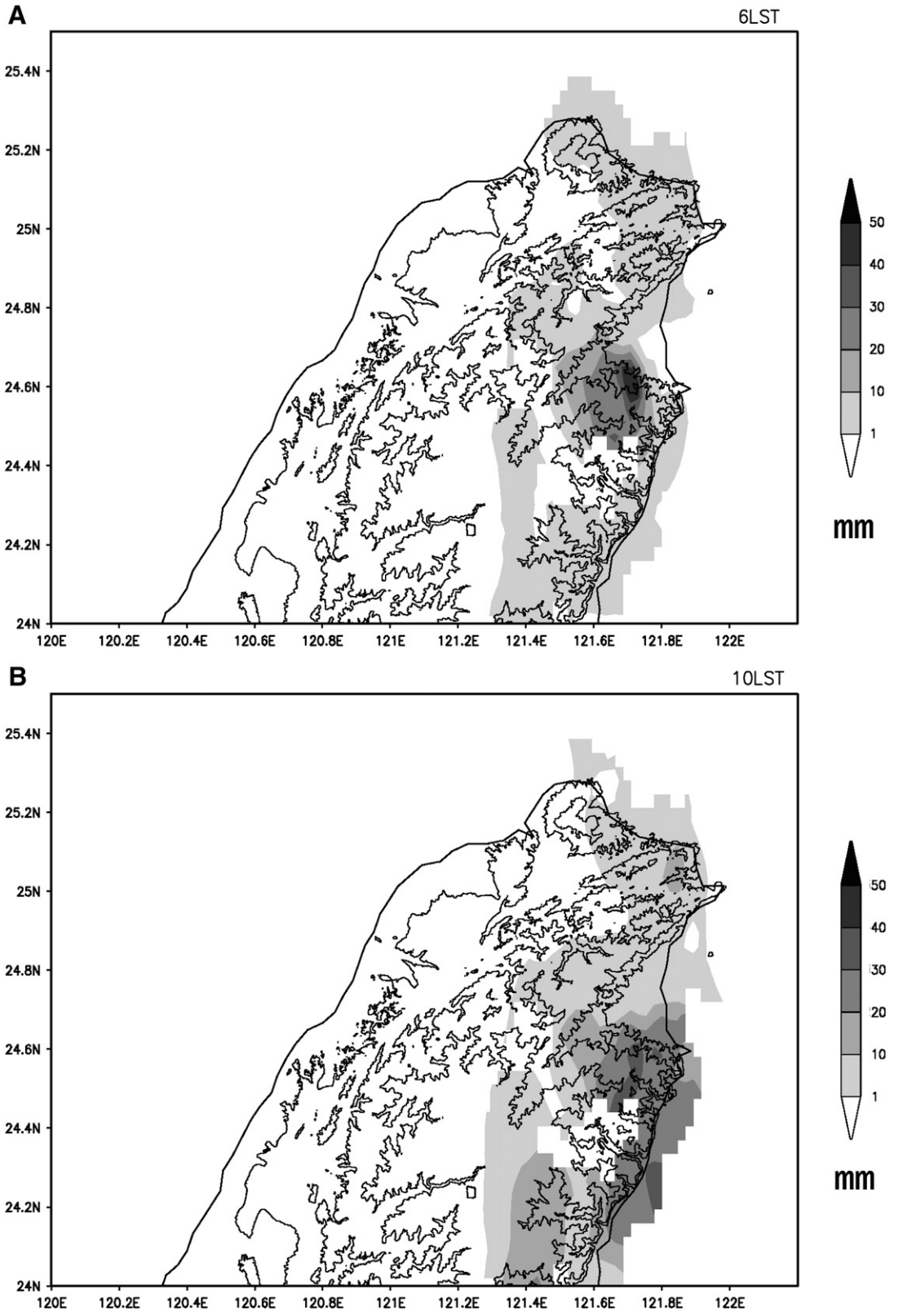

Fig. 7. The observed hourly rainfall rate at (A) 0600, (B) 1000, and (C) 1200 LST on 11 October 2009. The magnitude is sown by the gray scale in mm h^{-1}. The rainfall data is from stations shown in Fig. 1 and plotted by "Grads" software. Terrain height (solid lines) is 100, 500, and 1000 m, respectively.

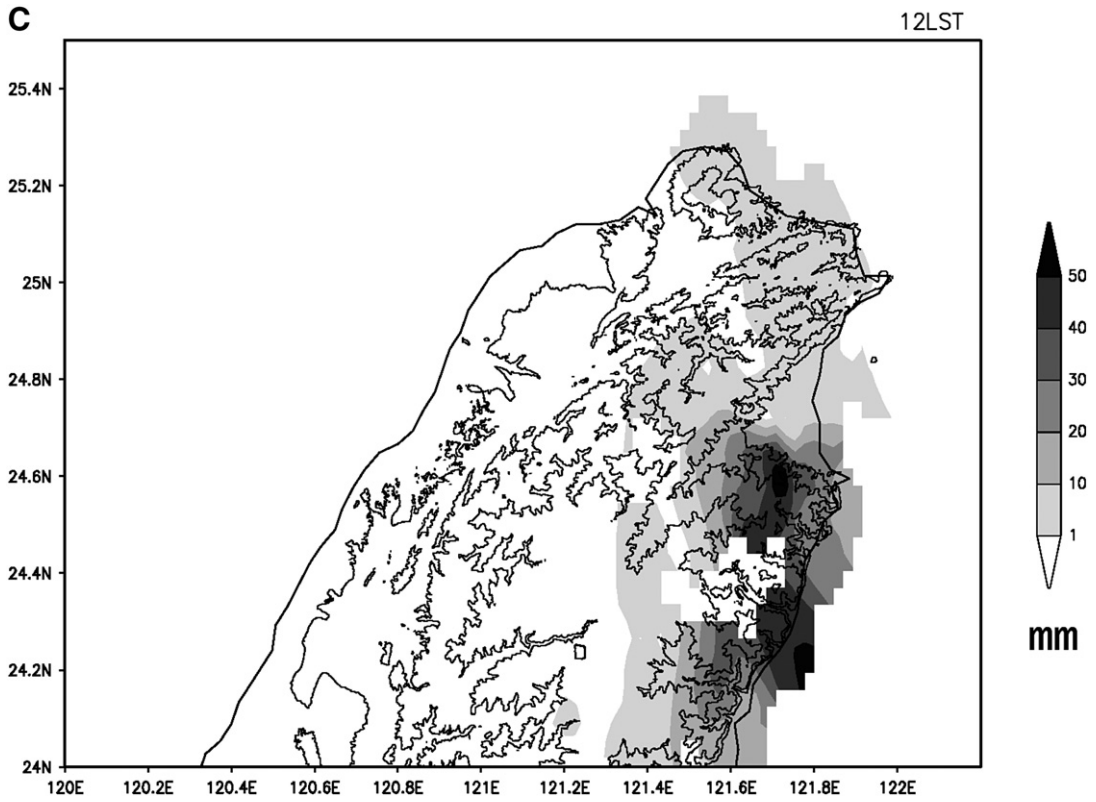

Fig. 7 (*continued*).

and a quasi-stationary rainfall system over the slope area result in a heavy rainfall event. The mechanism of producing heavy rainfall is consistent with Lin (2007).

The high rainfall rate over the slope area generates cool air (~121.81°E) at 1030 LST (Fig. 11E). The cool air interacts with the prevailing wind and enhances rainfall over a lower slope area. At 1100 LST, the cool air moves down the slope area towards the east (~121.87°E in Fig. 11F), as does the heavy rainfall area (~121.85°E). The eastward movement of rainfall is also evident in the temporal evolution of the east–west averaged simulated rainfall (1030~1100 LST and 121.81°~121.85°E in Fig. 10).

3.4. Impact of Taiwan's topography on the heavy rainfall over northeastern Taiwan

To isolate the effect of Taiwan's topography on the generation of heavy rainfall over northeastern Taiwan, we performed a sensitivity test with Taiwan's topography removed (the NT run). An east–west oriented rainband appeared in the confluent area between the easterly winds and the southeasterly winds (Fig. 12A) as in the control run (the CR run, Fig. 8B). Unlike the CR run, no contribution to the convergence (which could strengthen the east–west oriented rainband) was made by the deceleration of prevailing wind in the NT run. Note that the rainband was located slightly more to the south in the NT run compared to that in the CR run. Furthermore, no rainfall appeared over the slope area of northeastern Taiwan in the NT run, unlike that in the CR run. Relatively high accumulated rainfall over eastern Taiwan was apparently associated with the east–west oriented rainband. The simulated accumulated rainfall of the NT run over northeastern Taiwan was less than 50 mm in one day (Fig. 12B), much less than in the CR run (Fig. 9). The results from the NT run indicates that the heavy rainfall cannot be generated over northeastern Taiwan without orographic blocking and lifting effects despite the suitable synoptic circulations are present.

To examine the effect of orographic lifting over the slope south of the LYP on the production of heavy rainfall, a sensitivity test (the PL Run) was designed to reduce the orographic lifting by replacing the LYP with a plateau (Fig. 1C). At 0600 LST, the east–west oriented rainband located in the confluent area between the easterly winds and the southeasterly winds is simulated over east-central Taiwan (Fig. 13A), consistent with the CR run (Fig. 8B). In addition, the appearance of a high rainfall rate over the northeastern coast in the PL run is similar to the CR run. However, the rainfall rate over the inland of northeastern Taiwan is weaker in the PL run than in the CR run. The simulated daily rainfall in the PL run is heavy along the northeastern coast and the accumulated daily rainfall over the slope south of the LYP in the PL run is reduced by ~250 mm (Fig. 13B) compared to the CR run (Fig. 9).

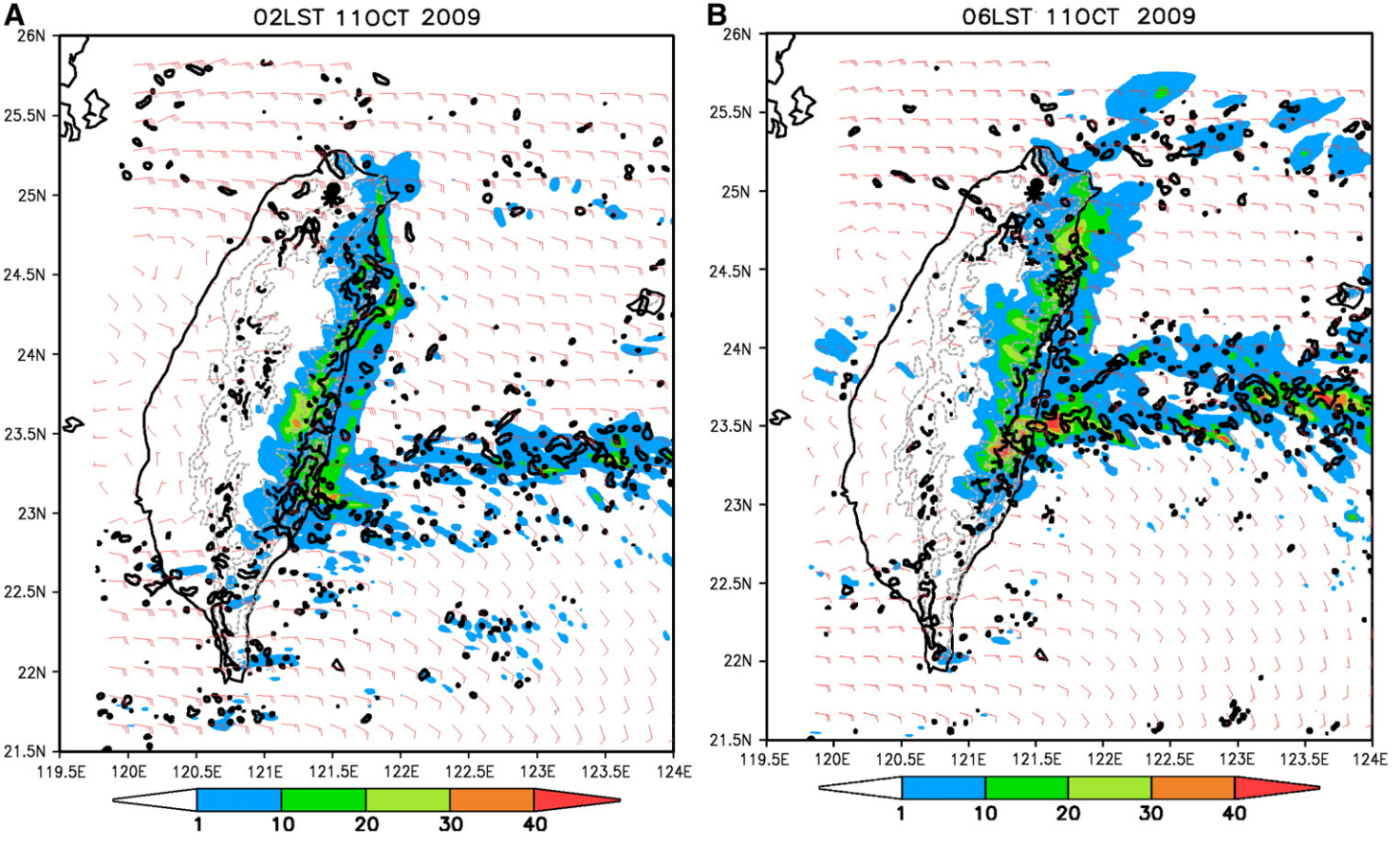

Fig. 8. The simulated hourly rainfall rate and 850-hPa wind from the 6- km grid spacing model. (a) 0200 (b) 0600 (c) 1100 LST on 11 October 2009. Rainfall rate is shown by the color scale (mm h^{-1}). The heavy black lines encircle the areas with convergence exceeding 10^{-3} s^{-1}. Terrain height (solid lines) is 500, 1000, and 1500 m, respectively.

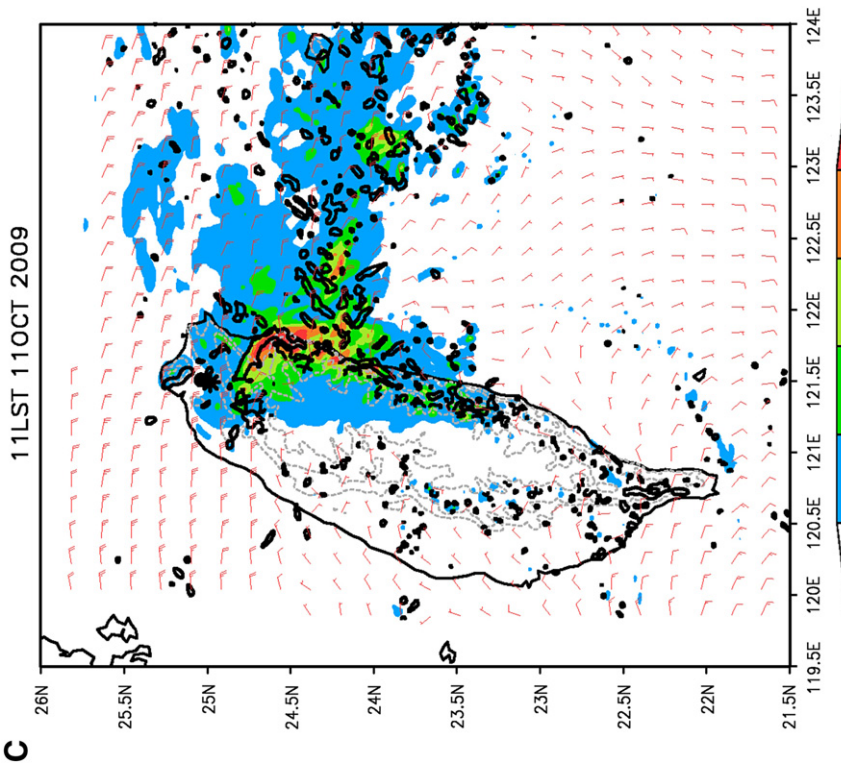

Fig. 8 (*continued*).

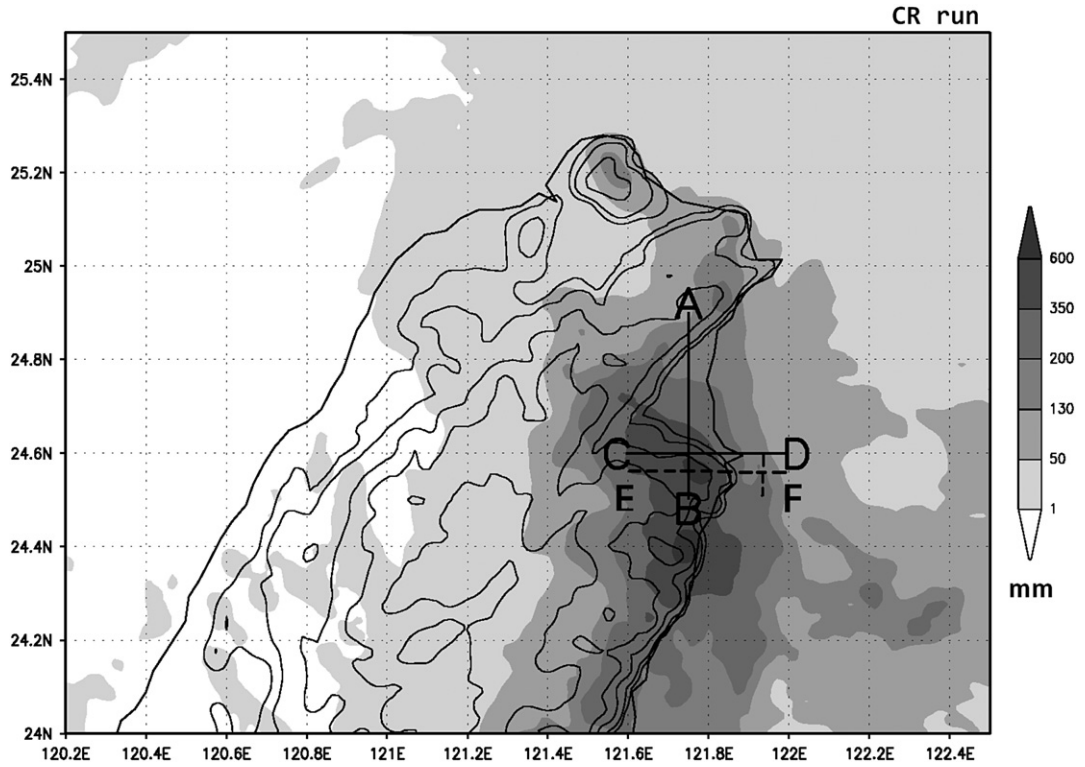

Fig. 9. The simulated daily accumulated rainfall obtained from the 2- km grid spacing model for the CR run. Rainfall amount is shown by the gray scale (mm). Lines AB and CD are used in Fig. 11. Line EF is used in Fig. 10. Line perpendicular to EF represents averaging width. Terrain height (solid lines) is 100, 200, 500, 1000, and 2000 m, respectively.

The reduction of rainfall is caused by lifting relatively dry air over the plateau where the surface elevation in the LYP (Fig. 1C) is higher than in the CR Run (Fig. 1B). In addition, the lifting of moist airstream associated with the prevailing easterly wind by the mountains is mainly over the coast (Fig. 13B). This result is different in the CR run, which was located further inland (Fig. 11D).

Apparently, the low-level convergence between the easterly wind and the southeasterly wind near northeastern Taiwan embedded in the synoptic-scale circulations is insufficient to initiate the heavy rainfall over northeastern Taiwan. The sensitivity tests indicate that the importance of orographic effects on the formation and maintenance of heavy rainfall over northeastern Taiwan. The enhancement of rainfall by the east–west oriented rainband is also demonstrated.

4. Summary

The orographic lifting and blocking effects on a heavy rainfall event occurred in northeastern Taiwan on 11 October 2009 during the northeasterly monsoon season were examined in this study. To the east (upstream side) of northeastern Taiwan, the low-level easterly wind over the East China Sea related to the high pressure system in east-central China converged with the southeasterly wind over the western North Pacific Ocean, which was associated with the monsoon trough/ITCZ. No synoptic disturbance was found within 500 km of northeastern Taiwan. In addition, over the South China Sea (SCS), the westward-movement of Typhoon Parma enhanced the southeasterly wind over the western Pacific Ocean. Thus, the low-level convergence over the ocean near northeastern Taiwan and the transport of moisture to northeastern Taiwan were enhanced, as shown in the schematic diagram (Fig. 14A).

Radar echoes occurred over northeastern Taiwan frequently on 11 October, especially over the slope areas. In addition, an east–west oriented rainband moved northward from the southeastern Taiwan and reached northeastern Taiwan around 1000 LST. Due to the persistence of the occurrence of radar echoes exceeding 20 dBZ over the slope south of the LYP, the maximum occurrence frequency of radar echoes for the whole day was greater than 50% over there. The high frequency of the occurrence of radar echoes over the slopes south of the LYP resulted in heavy rainfall in situ. The maximum accumulated daily rainfall of 631.5 mm was located about 5 km to the northwest of the maximum occurrence of radar echoes.

The WRF model was employed to examine the orographic effects on the generation and maintenance of this particular heavy rainfall event over northeastern Taiwan in the environment characterized by low moist Froude number (0.55). Because of the orographic blocking on the prevailing easterly wind over the western LYP, the induced near-surface northeasterly flow with moist airstream was lifted over the windward (south) side of the LYP and rainfall was generated in situ, as shown in the schematic diagram (Fig. 14B).

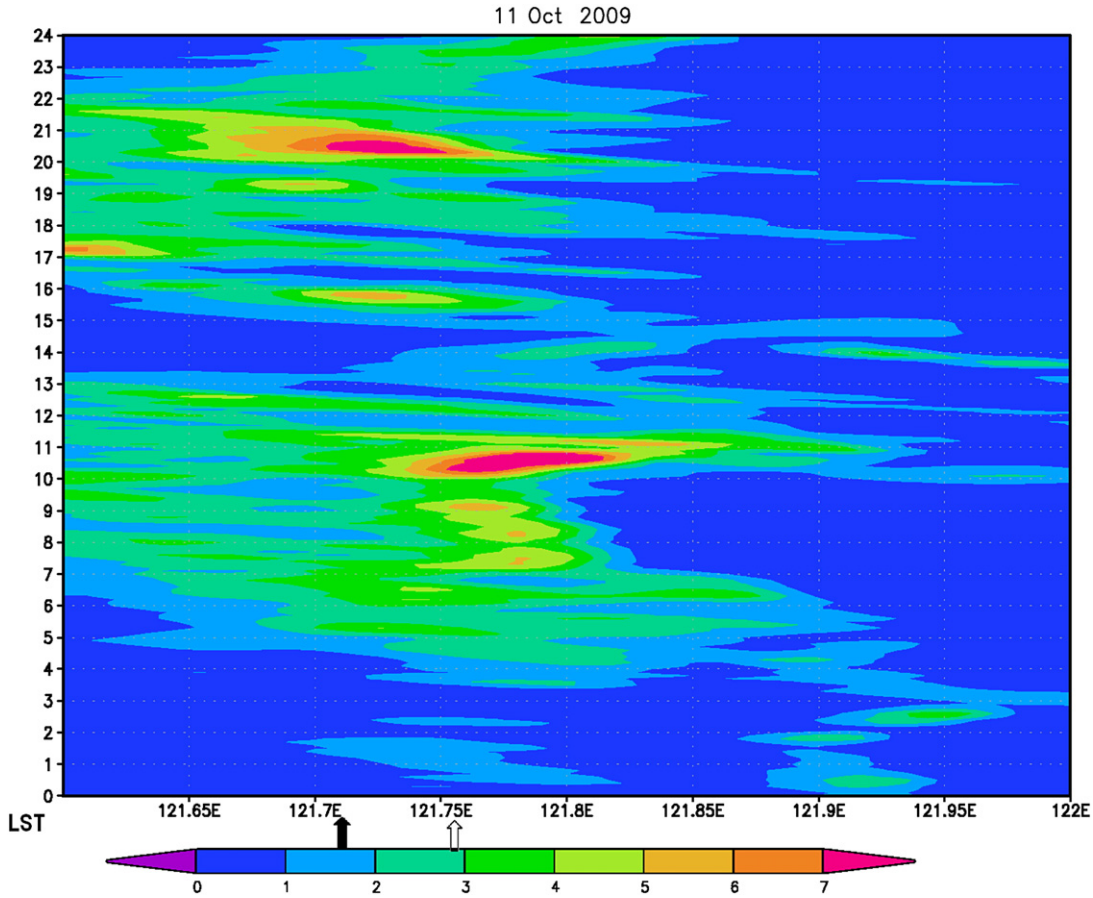

Fig. 10. The temporal evolution of the averaged simulated rainfall in a 10- km averaging width along EF in Fig. 9 obtained from 2 km grid spacing model for the CR run. The open (closed) arrow represents the approximate location of the maximum simulated (observed) daily accumulated rainfall.

Meanwhile, the simulated rainfall was embedded in a weak midtropospheric flow with the wind reversing its direction over the windward side of the LYP, resulting in a quasi-stationary precipitation system over a slope area. Furthermore, the prevailing easterly wind ascended over the coastal slope south of the LYP and enhanced the rainfall there (Fig. 14B). In addition, the approaching east–west oriented rainband from southeastern Taiwan also strengthened the rainfall intensity over northeastern Taiwan. Because the synoptic features (Fig. 14A) changed slowly on 11 October, the mesoscale features resulting in heavy rainfall were maintained over the slope south of the LYP for a relatively longer time period.

The sensitivity experiment with Taiwan's topography removed (the NT run) shows that the simulated accumulated daily rainfall over northeastern Taiwan in the NT run was less than 50 mm, much less than in the CR run even though the simulated rainband still approached northeastern Taiwan, similar to the CR run. Another sensitivity experiment (the PL run) with the LYP replaced by a plateau (Fig. 1C) shows that the accumulated daily rainfall over the slope south of the LYP was reduced by ~250 mm compared to the CR run. The reduction of rainfall was caused by the lifting of relatively less moist air over the slope south of the LYP. This demonstrates that the low-level convergence between the easterly wind and the southeasterly wind near northeastern Taiwan embedded in the synoptic-scale circulations was inadequate to trigger and maintain the heavy rainfall over northeastern Taiwan. Thus we may conclude that the orographic effects play a crucial role on the formation and maintenance of heavy rainfall over northeastern Taiwan.

Fig. 11. Simulated rainwater (solid line in g kg^{-1}), ascending motion exceeding 0.5 m^{-1} (shaded areas), water vapor mixing ratio (dotted lines with 1 g kg^{-1} interval) and along cross section winds from the CR run with 2-km grid space on the vertical cross section along line AB (Fig. 9) at: (a) 0600 and (b) 1000 LST. (c) Simulated rainwater (solid line in g kg^{-1}), ascending motion exceeding 1 m^{-1} (shaded areas), the saturated equivalent potential temperature (red lines in K), relatively humidity (green lines at 99 and 95 %) and along cross section winds from the CR run with 2-km grid space on the vertical cross section along line CD (Fig. 9) at 0600 LST. (d) Same as (b) but for cross section along line CD. Simulated rainwater (solid lines in g kg^{-1}), virtual potential temperature (dotted lines with interval of 1 K) and along cross section winds from the CR run with 2- km grid space on the vertical cross section along line CD (Fig. 9) at: (e)1030 LST and (f) 1100 LST. The triangles in (c)-(f) denote the coast. The open arrows in (a)-(f) represent the approximate locations of the simulated maximum accumulated daily rainfall. The terrains shown at bottom of each panel are smoothed.

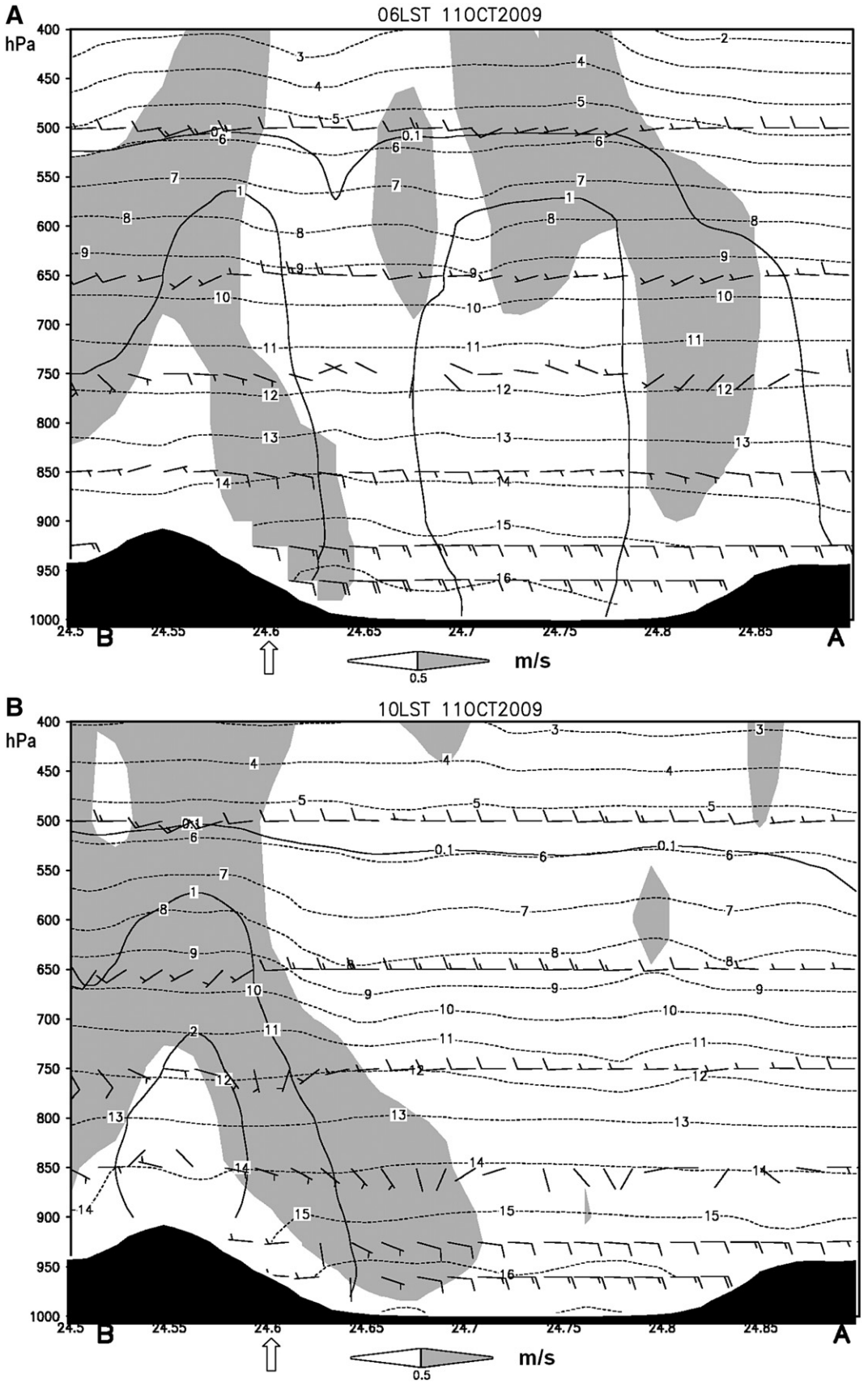
A
06LST 11OCT2009
hPa
400
450
500
550
600
650
700
750
800
850
900
950
1000
24.5
24.55
24.6
24.65
24.7
24.75
24.8
24.85
B
A
m/s
0.5
B
10LST 11OCT2009
hPa
m/s
0.5

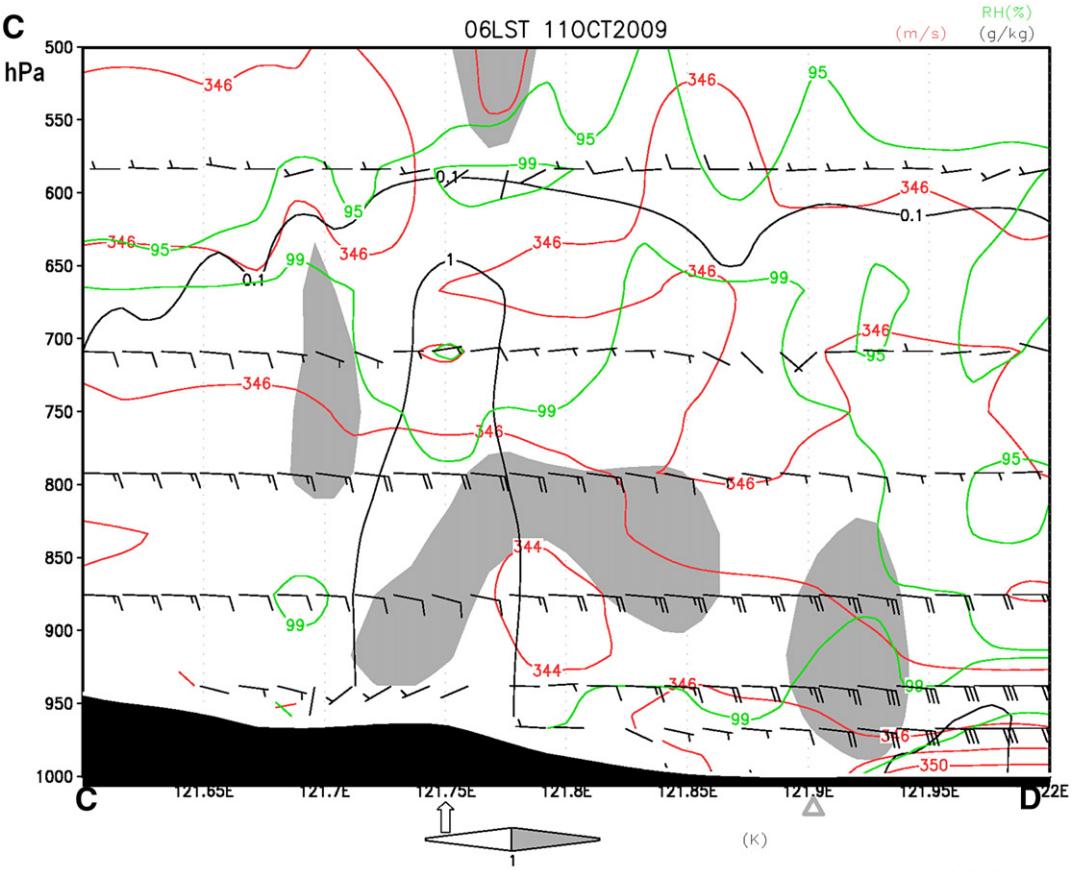
C
06LST 11OCT2009
RH(%)
(m/s)
(g/kg)
hPa
500
550
600
650
700
750
800
850
900
950
1000
346
95
99
0.1
1
344
350
C
121.65E
121.7E
121.75E
121.8E
121.85E
121.9E
121.95E
D
122E
1
(K)

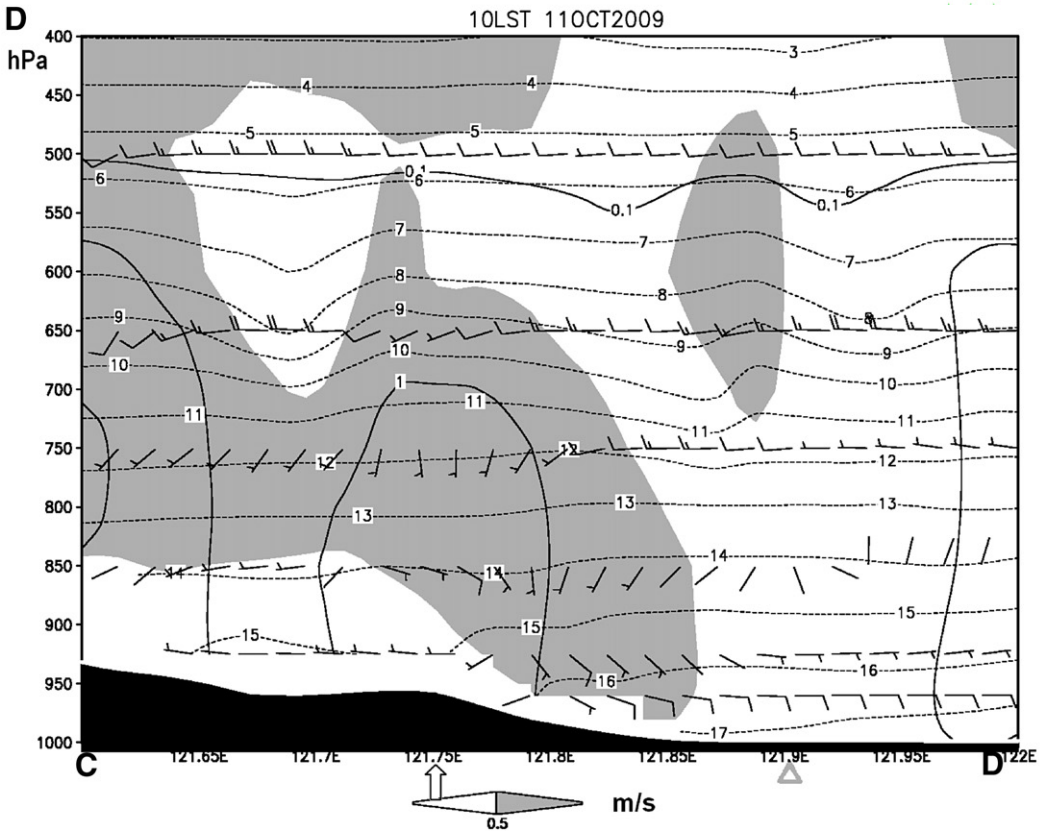
D
10LST 11OCT2009
hPa
400
450
500
550
600
650
700
750
800
850
900
950
1000
3
4
5
6
0.1
7
8
9
10
1
11
12
13
14
15
16
17
C
121.65E
121.7E
121.75E
121.8E
121.85E
121.9E
121.95E
D
122E
0.5
m/s

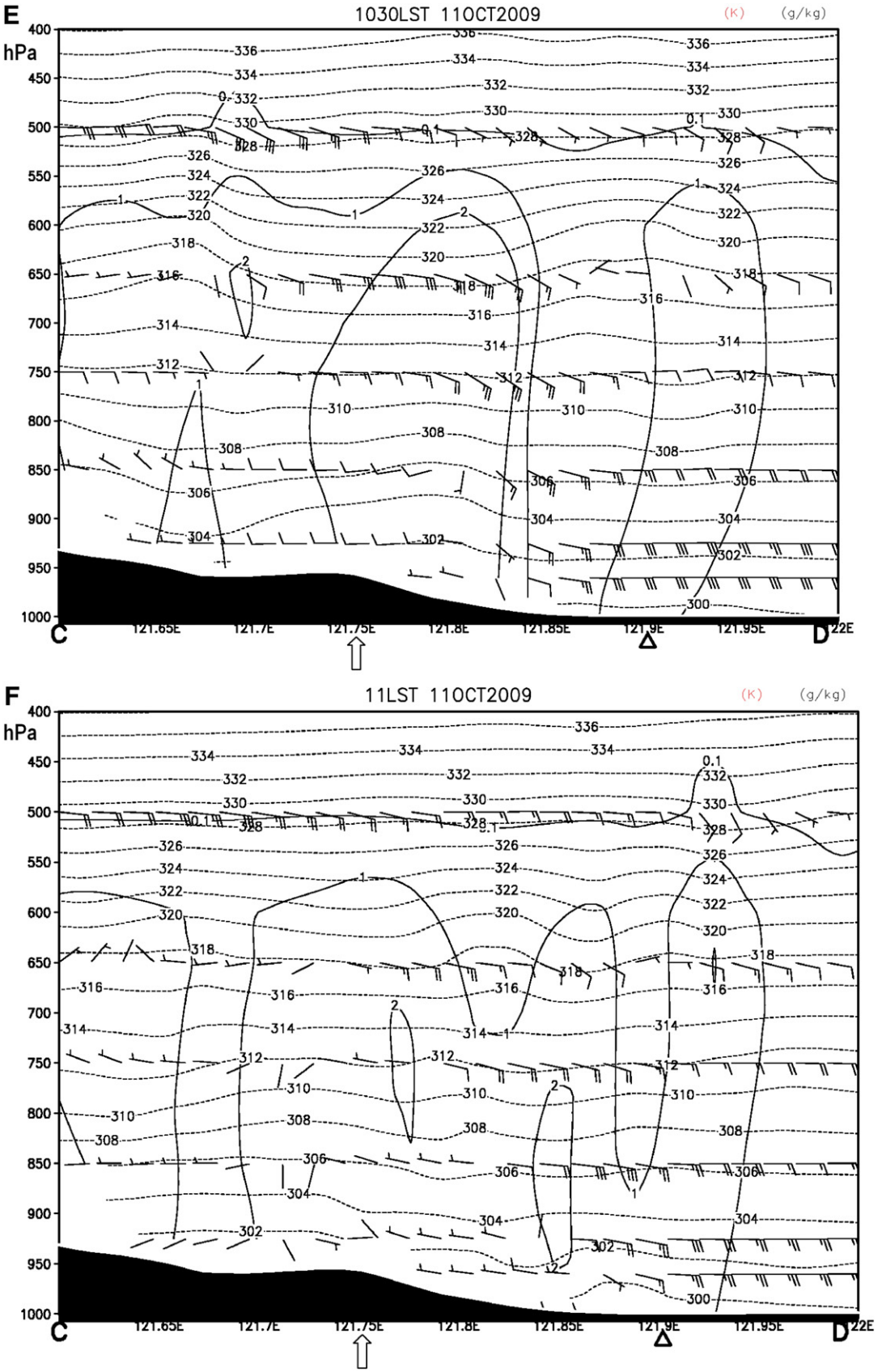
E
1030LST 11OCT2009
(K) (g/kg)
hPa
C
D
F
11LST 11OCT2009
(K) (g/kg)
hPa
C
D

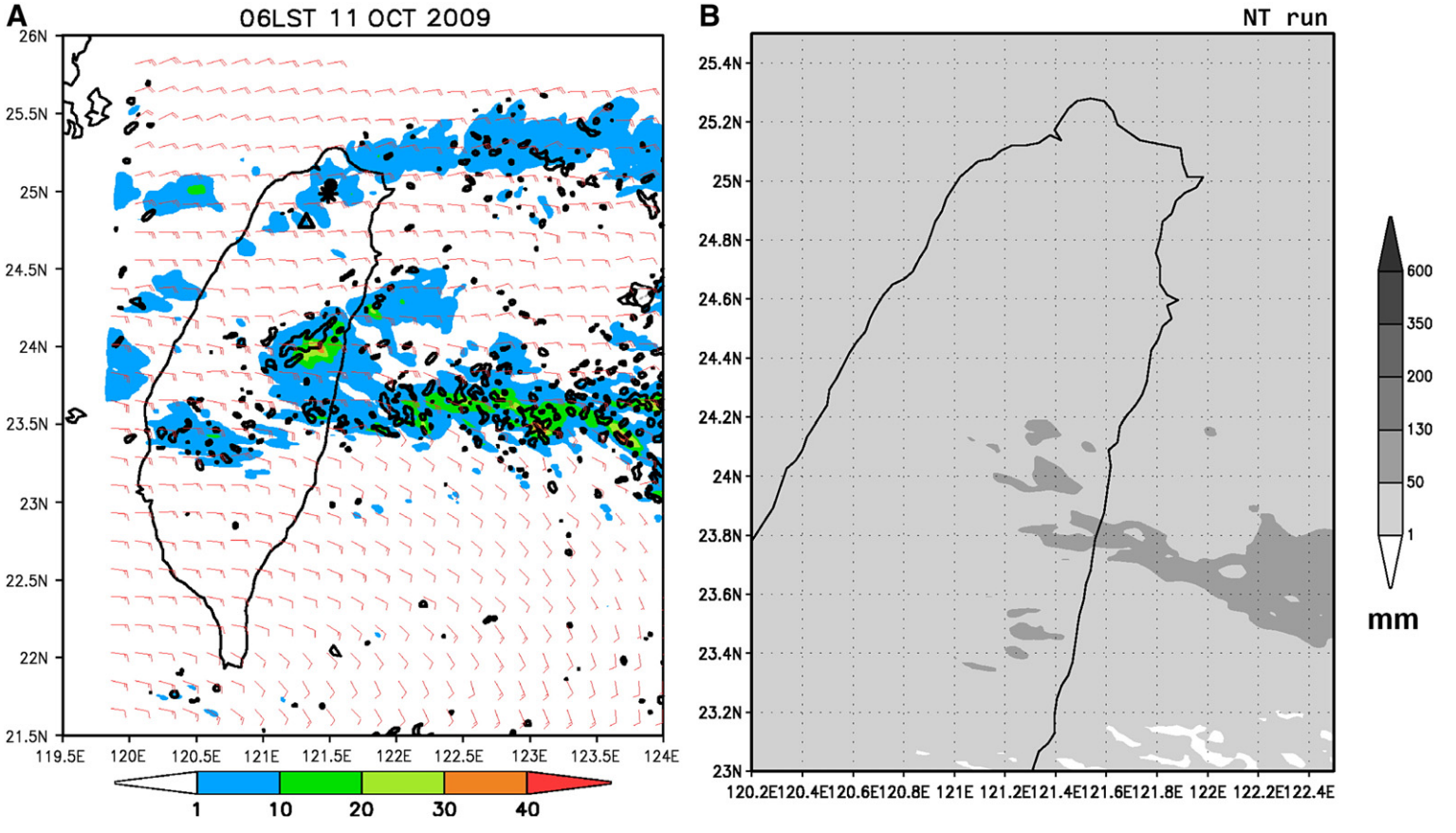

Fig. 12. (a) Same as Fig. 8b but for the NT run. (b) Same as Fig. 9 but for the NT run.

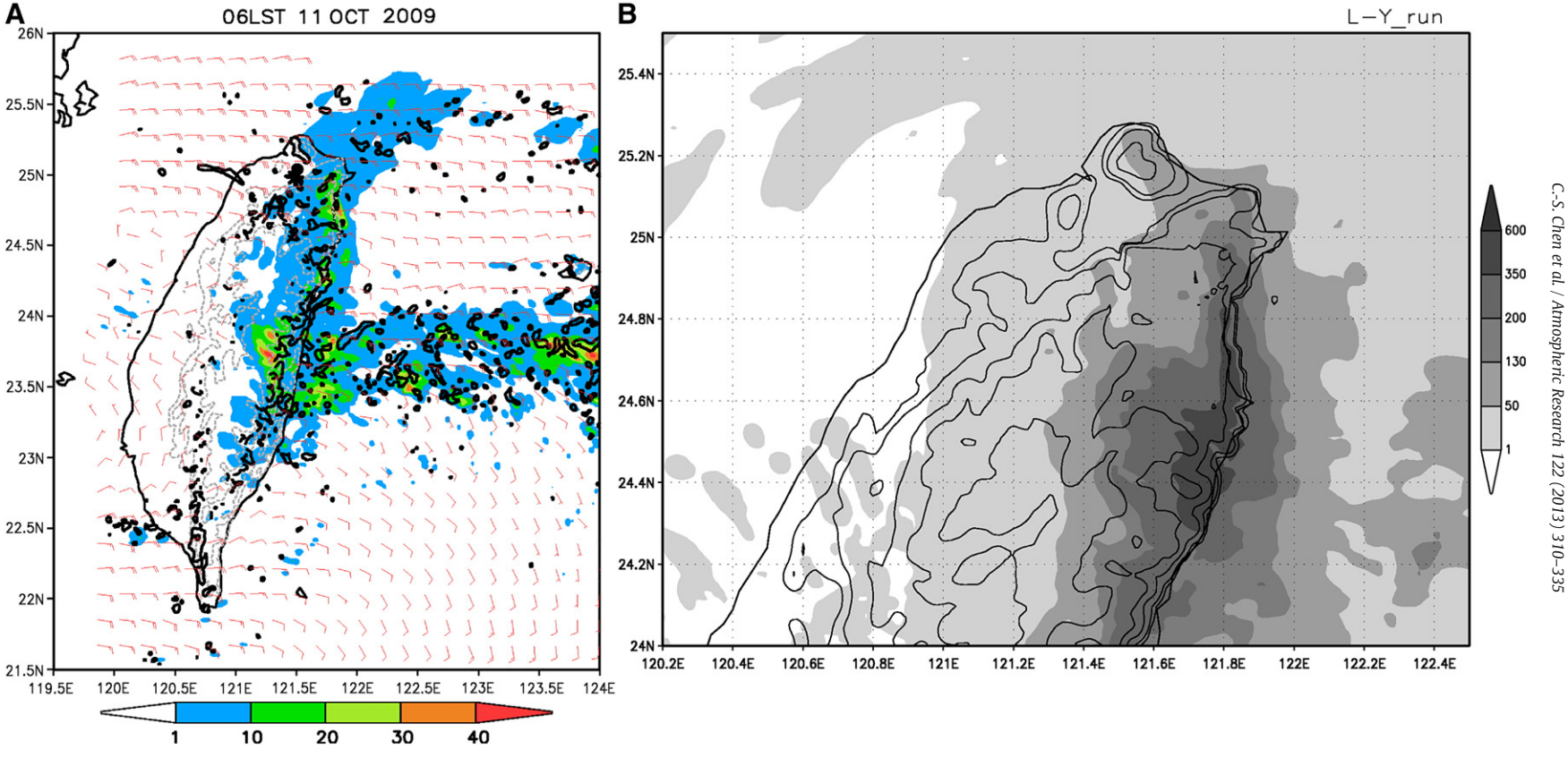

Fig. 13. (a) Same as Fig. 8b but for the PL run. (b) Same as Fig. 9 but for the PL run (see Fig. 1c).

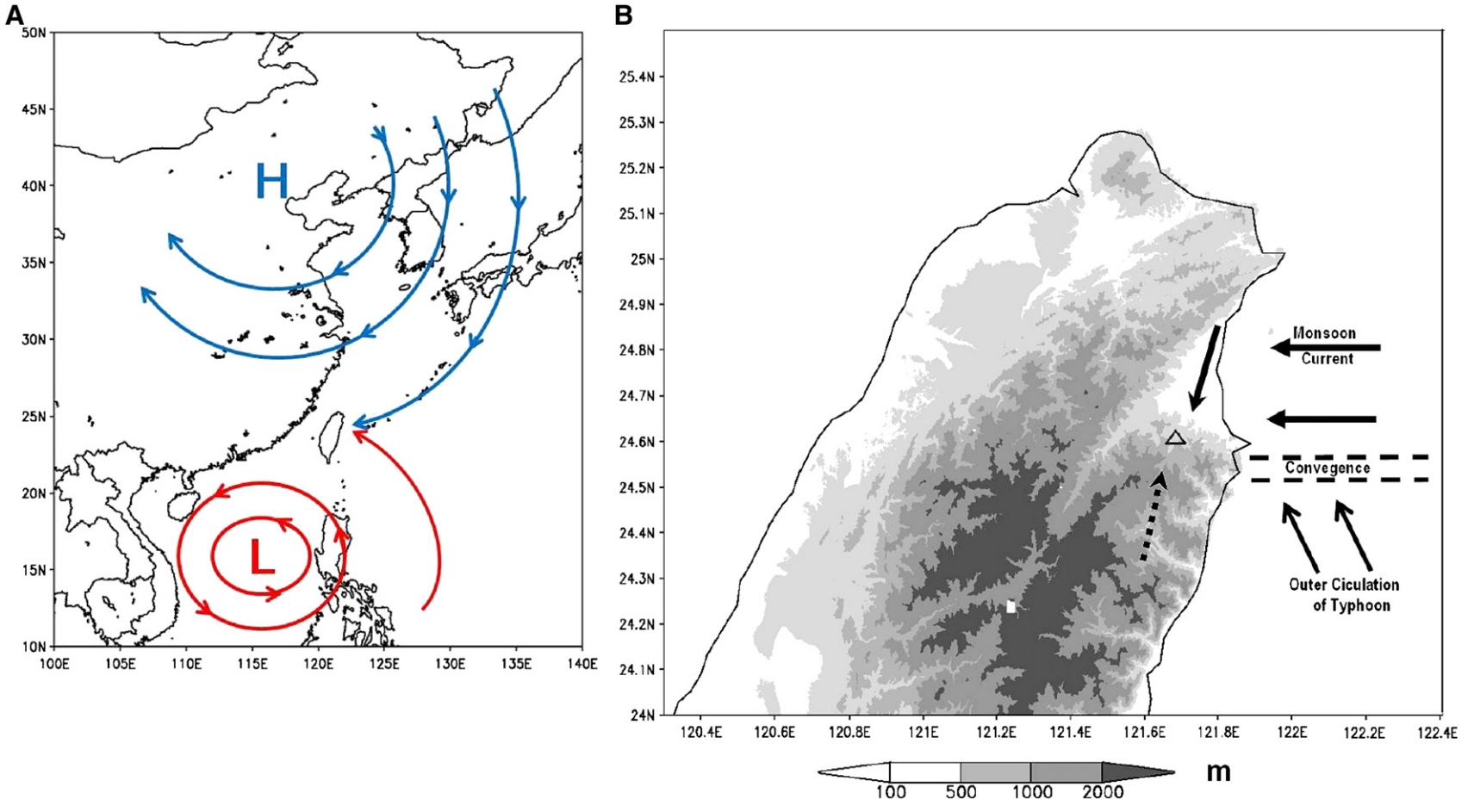

Fig. 14. (a) Schematic diagram for the environmental flow for the heavy rainfall event over northeastern Taiwan. H and L denote high pressure system and a typhoon over east-central China and the South China Sea, respectively. (b) Schematic diagram of the mesoscale flow features around the Lan-Yang Plain (LYP). The triangle denotes the location of the maximum accumulated daily rainfall. The solid and broken lines with arrow denote low-level and middle level winds, respectively. Two broken lines represent the convergence zone.

Acknowledgments

This work is supported by the National Science council of Taiwan under Grant NSC 100-2111-M-008-002 and the NOAA educational Partnership Program (EPP) under Cooperative Agreement NO: NA060AR4810187. We thank the Central Weather Bureau, Taipei, Taiwan, for providing the data. We would like to thank Michelle Lin for editing the text. The computer resources were supplied by the Center for computational Geophysics, National Central University, Chung-Li, Taiwan, under contribution number NCU-CCG100-0014.

References

Chen, C.-S., Chen, Y.-L., 2003. The rainfall characteristics of Taiwan. Mon. Weather Rev. 131, 1323–1341.

Chen, C.-S., Chen, W.-C., Chen, Y.-L., Lin, P.-L., Lai, H.-C., 2005. Investigation of orographic effects on two heavy rainfall events over southwestern Taiwan during the Mei-yu season. Atmos. Res. 73, 101–130.

Chen, C.-S., Lu, C.-H., Chen, W.-H., 2007a. Numerical experiments investigating the mechanisms of a heavy rainfall event over northeastern Taiwan and a mesovortex during TAMEX. Meteorol. Atmos. Phys. 95, 155–177.

Chen, C.-S., Chen, Y.-L., Liu, C.-L., Lin, P.-L., Chen, W.-C., 2007b. Statistics of heavy rainfall occurrences in Taiwan. Weather Forecast. 22, 981–1002.

Chen, C.-S., Lin, Y.-L., Peng, W.-C., Liu, C.-L., 2010a. Investigation of a heavy rainfall event over southwestern Taiwan associated with a subsynoptic cyclone during the 2003 Mei-Yu season. Atmos. Res. 95, 235–254.

Chen, C.-S., Liu, C.-L., Yen, M.-C., Chen, C.-Y., Lin, P.-L., Huang, C.-Y., Teng, J.-H., 2010b. Terrain effects on an afternoon heavy rainfall event, observed over northern Taiwan on 20 June 2000 during monsoon break. J. Meteorol. Soc. Jpn 88, 649–671.

Chen, C.-S., Lin, Y.-L., Hsu, N.-N., Liu, C.-L., Chen, C.-Y., 2011. Orographic effects on localized heavy rainfall events over southwestern Taiwan on 27 and 28 during the Post-Mei-Yu season. Atmos. Res. 101, 595–610.

Chiao, S., Lin, Y.-L., Kaplan, M.L., 2004. Numerical study of the orographic forcing of heavy precipitation during MAP IOP -2B. Mon. Weather Rev. 132, 2184–2203.

Chu, C.-M., Lin, Y.-L., 2000. Effects of orography on the generation and propagation of mesoscale convective systems in a two-dimensional conditionally unstable flow. J. Atmos. Sci. 37, 3817–3837.

Dudhia, J., 1996. A mutil-layer soil temperature model for MM5. Preprints, Sixth PSU/NCAR Mesoscale model Users' Workshop, Boulder, Co, pp. 49–50 (Available online at http://www.mmm.ucar.edu/mm5/mm5v2/whatisnewinv2.html).

Federico, S., Avolio, E., Pasqualoni, L., De Leo, L., Sempreviva, A.M., Bellecci, C., 2009. Preliminary results of a 30-year daily rainfall data base in southern Italy. Atmos. Res. 94, 641–651.

Feng, Y.-C., Wang Chen, T.-C., 2011. Precipitation characteristics for an autumn torrential rainfall event in northern Taiwan as determined from Dual-Polarization radar data. J. Meteorol. Soc. Jpn 89, 133–150.

Janjic, Z.I., 1996. The surface layer in the NCEP Eta model. Preprints, Eleventh Conference on Numerical Weather Prediction. Norfolk. VA, 19–23 August. Amer. Meteor. Soc, Boston, MA, pp. 354–355.

Janjic, Z.I., 2002. Nonsingular Implementation of the Mellor-Yamada level 2.5 Scheme in the NCEP Mesoscale model. NCEP Office Note. No. 437. (61 pp.).

Kain, J.S., Fritsch, J.M., 1993. Convective parameterization for mesoscale models: The Kain-Fritsch scheme. The Representation of Cumulus Convection in Numerical Models. Meteorol. Monogr., No. 46. Am. Meteorol. Soc. 24, 165–170.

Li, J., Chen, Y.-L., Lee, W.-C., 1997. Analysis of a heavy rainfall event during TAMEX. Mon. Weather Rev. 125, 1060–1082.

Lin, Y.-L., 2007. Mesoscale Dynamics. Cambridge University Press, New York . (630 pp.).

Lin, C.-Y., Chen, C.-S., 2002. A study of orographic effects on mountain-generated precipitation systems under weak synoptic forcing. Meteorol. Atmos. Phys. 81, 1–25.

Lin, P.-L., Chen, Y.-L., Chen, C.-S., Liu, C.-L., Chen, C.-Y., 2011. Numerical experiments investigating the orographic effects on a heavy rainfall event over the northeastern coast of Taiwan during TAMEX IOP 13. Meteorol. Atmos. Phys. 114, 35–50.

Mastrangelo, D., Horvath, K., Riccio, A., Miglietta, M.M., 2011. Mechanisms for convection development in a long-lasting heavy precipitation event over southeastern Italy. Atmos. Res. 100, 586–602.

Skamarock, W.C., Klemp, J.B., Dudhia, J., Gill, D.O., Barker, D.M., Wang, W., Powers, G., 2005. A description of the Advanced Research WRF version 2. NCAR Tech. Note TN-468+STR. (88 pp. Available from NCAR, P.O. Box 3000, Boulder, CO 80307).

Tao, W.-K., Simpson, J., Baker, D., Braun, S., Chou, M.D., Ferrier, B., Johnson, D., Khain, A., Lang, S., Lynn, B., Shie, C.L., Starr, D., Sui, C.H., Wang, Y., Wetzel, P., 2003. Microphysis, radiation and surface processes in the Goddard Cumulus Ensemble (GCE) model. Meteorol. Atmos. Phys. 82, 97–137.

Wapler, K., Lane, T., 2012. A case of offshore convective initiation by interacting land breezes near Darwin, Australia. Meteorol. Atmos. Phys. 115, 123–137.

Wu, C.-C., Cheung, K.K.-W., Lo, Y.-Y., 2009. Numerical study of the rainfall event due to the interaction of Typhoon Babs (1998) and the Northeasterly monsoon. Mon. Weather Rev. 137, 2049–2064.

Yen, M.-C., Chen, C.-C., Hu, H.-L., Tzeng, R.-Y., Dinh, D.T., Nguyen, T.T.T., 2011. Interannual variation of the fall rainfall in central Vietnam. J. Meteorol. Soc. Jpn 89, 259–270.

Zeng, H.-T., 2011. A preliminary study of orographic effects on heavy autumn rainfall over northeastern Taiwan: A case study on 11 October 2009. MS thesis (In Chinese), NCU, Chung-Li, Taiwan, 83 pp.